ABSTRACT

Title of dissertation: MATHEMATICAL AND MOLECULAR STUDIES OF FELINE ERYTHRO-AND LYMPHOPOIESIS

Bren S Ewen, Master of Science, 2005

Dissertation directed by: Dr. Carol Pontzer, Department of Cell Biology and Molecular Genetics

Feline leukemia virus, strain KT, is a retrovirus that causes a fatal erythroid aplasia. The fatal loss of erythrocytes is due to the interaction of this virus with the BFU-E stage of feline erythropoietic development. This virus is comparable to the human HTLV retrovirus. Through the development of a computer mathematical model, we demonstrate the disease process and show that infection of the BFU-E leads to a characteristic fatal erythroid aplasia in cats.

Fetal feline lymphohematopoietic stem cells, before a certain point in gestation, lack genotypically unique class I major histocompatibility cell-surface antigens (FLA). The elucidation of a gestational time point when FLA appear on the surface of cells within the fetal liver will provide knowledge of when hematopoietic stem cells may be at maximal utility for gene therapy of feline hematopoietic disease,

specifically FIV. Here we show that this time point occurs around day 40 in fetal feline gestation.

MATHEMATICAL AND MOLECULAR STUDIES OF FELINE ERYTHRO- AND LYMPHOPOIESIS

by

Bren S Ewen

Thesis submitted to the Faculty of the Graduate School of the
University of Maryland, College Park in partial fulfillment
of the requirements for the degree of
Master of Science
2005

Advisory Committee:

Professor Wenxia Song, Chair
Professor Sam Joseph
Professor Carol M. Pontzer

DEDICATION

To Ann Ewen, my dear mother, whose life taught me that I could weather any storm and survive any trial; and whose dedication to life helped me grasp hold of my dreams and make every moment of every day count.

To Pat Beacham, without whose help this research would not have been possible. I can never repay the debt I owe.

To Sadie Ann Ewen, whom saved my life.

ACKNOWLEDGEMENTS

I wish to acknowledge the work of Dr. E. A. Hoover, whose FeLV data was given to me for use in the construction of the mathematical model and made available for my use in publications of this research.

I wish to acknowledge the assistance of Dr. Rick Kohn in determining the proper modeling software and mathematical analysis equations for construction and testing the mathematical model.

I wish to acknowledge Dr. Ayalew Mergia and Dr. Milton Hernandez for assisting me to obtain a grant to support the work upon which this thesis is based.

I wish to acknowledge the assistance of Dr. Suresh Poosala for his help with the Tissue Array and Immunohistochemistry Procedures.

Table of Contents

LIST OF DATA TABLES

LIST OF FIGURES

Figure Number **Page**

LIST OF ABBREVIATIONS USED

1. AA – Aplastic Anemia
2. BFU-E – Burst Forming Unit-Erythroid
3. BMT- Bone Marrow Transplant
4. CFU-E – Colony Forming Unit-Erythroid
5. Diff – Differential Cell Count
6. DPI – Days Post Inoculation
7. EA – Erythroid Aplasia
8. FeLV – Feline Leukemia Virus
9. FeLV-AA – Feline Leukemia Virus induced Aplastic Anemia
10. FeLV-EA – Feline Leukemia Virus induced Erythroid Aplasia (also called FeLV-AA)
11. FeLV-KT – Feline Leukemia Virus, strain KT
12. FHSC – Fetal Hematopoietic Stem Cells
13. FIV – Feline Immunodeficiency Virus
14. FLA – Feline Major Histocompatibility Antigens
15. FOCMA – Feline Oncovirus-Associated Cell Membrane Antigen
16. FFU – Focus Forming Units
17. GCSF – Granulocyte-colony Stimulating Factor
18. GVHD – Graft-versus-host-disease
19. Hct. – Hematocrit or VPRC
20. HIV – Human Immunodeficiency Virus
21. HSC(s) – Hematopoietic Stem Cell(s)

22. HSCT – Hematopoietic Stem Cell Transplant

23. Kg - Kilogram

24. mg – milligram

25. ml – milliliter

26. MHC – Major Histocompatibility antigens

27. MPA – Methyl Prednisolone Acetate

28. ORFs – Open reading frames

29. RBC(s) – Red Blood Cell(s)

30. RMSPE – Root Mean Square Prediction Error

31. SPF – Specific Pathogen Free

32. VPRC – Volume of Packed Red Blood Cells

CHAPTER I:

Computer Modeling of Normal and Feline Leukemia Virus –Infected Feline Erythropoiesis

Overview and Significance

The Kawakami-Theilen strain of feline leukemia virus (FeLV-KT or FeLV-C)) is an exogenous anemia-inducing retrovirus. FeLV is the most important infectious disease agent producing fatal illness in domestic cats today. Additionally, its relation to the human HTLV virus makes it an attractive model for study of the pathogenesis of diseases related to infection with the virus. This knowledge will hopefully allow more insights into preventions and treatments for both FeLV infection in cats and HTLV infection in humans.

FeLV is excreted in saliva and tears, the urine and the feces of infected cats. Prolonged, extensive cat-to-cat contact is required for efficient spread because the virus is rapidly inactivated by warmth and drying. There are three main types of feline leukemia virus: FeLV-A, FeLV-B, and FeLV-C (FeLV-KT). FeLV-positive cats can be infected with one, two, or all three types:

1. FeLV-A occurs in all FeLV-infected cats and causes severe immunosuppression.
2. FeLV-B occurs in about 50% of all FeLV-infected cats and causes more neoplastic disease than cats infected only with FeLV-A.
3. FeLV-C, or FeLV-KT, occurs in about 1% of FeLV-infected cats and causes severe anemia.

After the initial infection, the virus replicates in the tonsils and pharyngeal lymph nodes. It then spreads via the bloodstream to other parts of the body, especially the lymph nodes, bone marrow, and intestinal tissue, where it continues to replicate. Viremia usually presents 2 to 4 weeks after the initial infection.

FeLV is one of the most devastating feline diseases worldwide. In the United States, FeLV infects about 2% to 3% of all cats. Cats ill from other acute or chronic disorders are four times more likely than healthy cats to be infected with FeLV. Researchers estimate that about 50% of cats with severe bacterial infections, and 75% of cats with toxoplasmosis also have FeLV infections.

FeLV-KT-Induced Erythroid Aplasia

Experimentally induced FeLV-erythroid aplasia is a fatal normocytic and normochromic anemia associated with bone marrow hypoplasia, lymphopenia, leukopenia and, less consistently, with myeloschlerosis.[4-6] Of the recognized strains of FeLV, only FeLV-KT isolates have been shown to induce FeLV-erythroid aplasia.[5-8] The FeLV virus targets the Burst Forming Unit-Erythroid (BFU-E) cells in the erythropoietic developmental pathway, blocking the production of fully mature red blood cells. It has been speculated that FeLV-KT might arise de novo in cats with FeLV-A viremia, perhaps as a recombinant of FeLV-A and endogenous cellular DNA sequences.[9-10] Although the association of marrow aplasia with FeLV-KT is known, the pathogenesis of the virus has remained unclear.

Mathematical Modeling of Normal Feline Erythropoiesis

Specific Aims

To begin to study the pathogenesis of FeLV-KT using a mathematical model, it is important to first construct a working model of normal erythropoiesis, to verify that such a model can predict the outcomes of real-time feline erythropoiesis.

Rationale

In order to create a realistic and useful model for the examination of FeLV-KT infection and subsequent red cell aplasia, the model must first be able to mimic normal feline erythropoiesis. Because we hope to show that the infection by FeLV-KT causes a characteristic loss of red cells, it is important that any model, developed adequately and accurately, demonstrate the normal development of these cells. The influential factors include the number of changes, mitoses and different time values these cells undergo to produce a steady state of $1x10^9$ RBCs.

Materials and Methods

Mathematical Modeling

Development of a precise model of normal erythropoiesis will provide the opportunity for the perturbation of this system and the targeted placement of FeLV-KT at the level of the fifth mitotic stage of BFU-E development. The successful development of this model will support the real system data, demonstrating a characteristic slope produced by the loss of Hct.

Stella 5.1.1, Research Version, created by High Performance Systems, Inc., was the software utilized for the construction of both normal and FeLV-KT-infected feline erythropoiesis. This software has many benefits over other types on the market, in that it is amenable to the incorporation of data and real system outputs from bench experiments and automatically assigns differential equations to the expressions created within the model layer. Before the discussion of the mathematical model can begin, the elements used in the creation of this prototype must first be defined in order for the reader to have a clear understanding of the construction of our representation of erythropoiesis.

There are three map layers found within the model: 1.The High-Level Map Layer 2.The Model Layer 3. The Equation Layer.

The High Level Map layer displays the essential actors or the overall picture found within the model layer (Fig. 1). Here we not only show the big picture but the interaction of each major player with the other. The three aspects that we have determined to constitute the predominate parts of erythropoiesis are:

- feline hematopoietic stem cells
- the erythropoietic development pathway
- circulating mature red blood cells.

The model layer is where the true workings are found. This section is composed of the major cell compartments found in our model. Within each compartment, the

principle part of modeling occurs. It is necessary to define the tools used in the formation of our erythropoietic representation.

The first tool used in the development of our model was the stock. The stock can carry out 4 distinct mathematical functions, depending on the device chosen. Two different types were used; a reservoir, which allowed a certain number of items, in our case these are cells, to remain within the stock. The second stock device used was the conveyor. A conveyor, representing the cell compartment, allowed items to flow into it, stay a certain amount of time, carry out certain functions, i.e. divide or mature, and then leave after that end time point is reached.

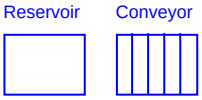

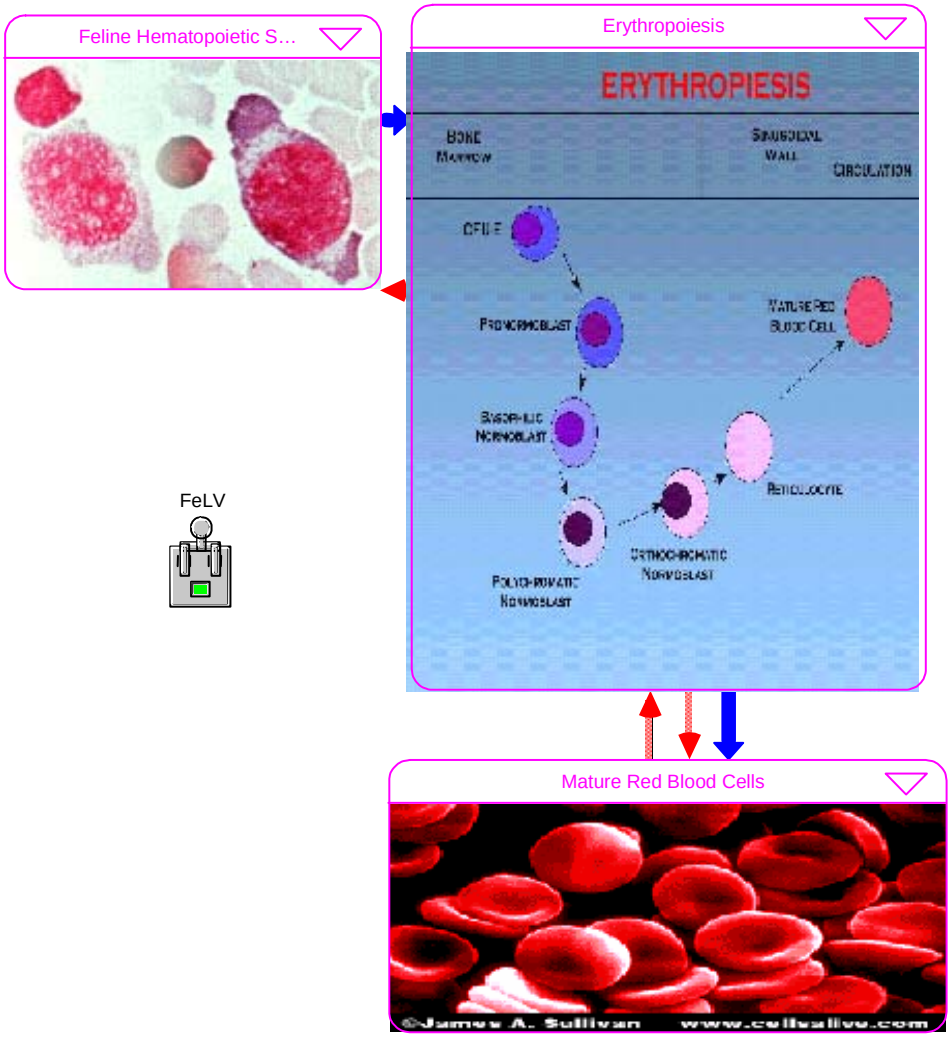

Figure 1. High-Level Map Layer. The first layer of the mathematical model allows for the connection of the secondary mathematical modeling level, as well as

providing switches for special effects, in this case the virus of interest, Feline Leukemia Virus-KT.

The second tool applied to the model was the flow. The purpose of the flow is to fill and to drain accumulations. In the model of erythropoiesis, these flows carry the cells from one compartment, or stock, to another. The unfilled arrowhead on the flow pipe indicates the direction of flow. The "cloud" at the beginning of the flow merely represents the fact that the items are not moving from any out side source, or are originating and controlled by the stock into which they flow.

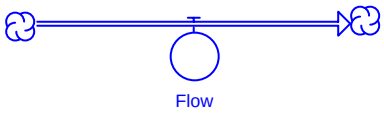

A third tool employed was the converter, which will be discussed in the next experimental section dealing with the creation of FeLV-KT-infected erythropoiesis.

The last major tool, important to the Model Layer development, is the connector. The connector was used to connect model elements, such that the element from where the connector originated controlled or directed the movement of the cells in the item to which the connector pointed. In the example below, the red arrows are the connectors. These arrows signify that the differentiation fraction and the hematopoietic stem cells control erythropoietic differentiation. When a model element is opened, by double clicking using a computer mouse, a dialog box opens allowing the modeler to write

an equation. In the example shown the equation would be:

Hematopoietic_Stem_Cells*Differentiation_Fraction

The actual equation is 8 (Hematopoietic Stem Cells) multiplied by 1/8 (Differentiation Fraction) so that only one stem cell undergoes erythropoietic differentiation at any one time under the conditions of normal erythropoietic development.

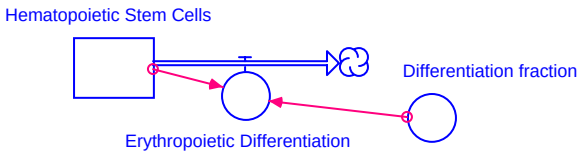

When constructing the FeLV-infected computer model, we "transplanted" 8 hematopoietic stem cells into the system, allowing one HSC to give rise to a total of 10^9 mature red cells or packed red cells. The number of stem cells was determined as it has been demonstrated in mice, cats, dogs and primates, that only 8 stem cells are required to repopulate the lymphohematopoietic architecture.[18] The pathway was modeled in log scale to give a biologically correct analysis of the synthetic system. Both the BFU-E and CFU-E cell compartments contained 5 distinct mitoses. The cell(s) multiplied by a factor of 1.584893192, within each mitosis, to simulate actual biological events, as suggested by Wichmann and Loeffler.[11]

We will explore the discussion of FeLV viral control within the model in the next section. Briefly, certain expressions enabled a toggle switch, which was connected from the High Level Map layer to a converter representing FeLV on the model layer,

to control the presence and absence of FeLV, subsequently controlling feline stem cells and BFU-E cells and further impacting all cell compartments along the erythropoietic differentiation pathway. The virus either infected the BFU-E cells (toggle switch returned a value of 1 and was turned on; virus was present), stopping further division and causing cell death or was absent from the cells (toggle switch returned a value of 0 and was turned off). The loss of BFU-E cells and VPRCs, as well as the shift of HSCs to the erythropoietic pathway, were then analyzed through the software's graphical and animation utilities.

One of the major benefits of using the Stella software package was the automatic assignment of differential equations to each part of the diagram. In calculus parlance, the software used flows to represent time derivatives; stocks were the integrals (or accumulations) of flows over time; converters contained the micro-logic of flows.

Results

As a first step, we designed a model to imitate normal, feline erythropoietic development (Figure 2). It is known that between the BFU-E stage and the reticulocyte stage, there is a 5-fold increase in the cell numbers. There are 5 distinct mitoses that take place within the BFU-E compartment. The average time for a cell to under go all 5 is 24 hours. Additionally, it takes an average of 8 hours for a cell entering the CFU-E stage of development to undergo all 5 CFU-E distinct mitoses.[11-12] It is also known that complete feline erythropoietic development requires an average of 70 days.[13] These facts were incorporated into our model setup to ensure

biological authenticity. The end result of this model was that one HSC gave rise to 10^9 red blood cells and the model maintained a steady state.

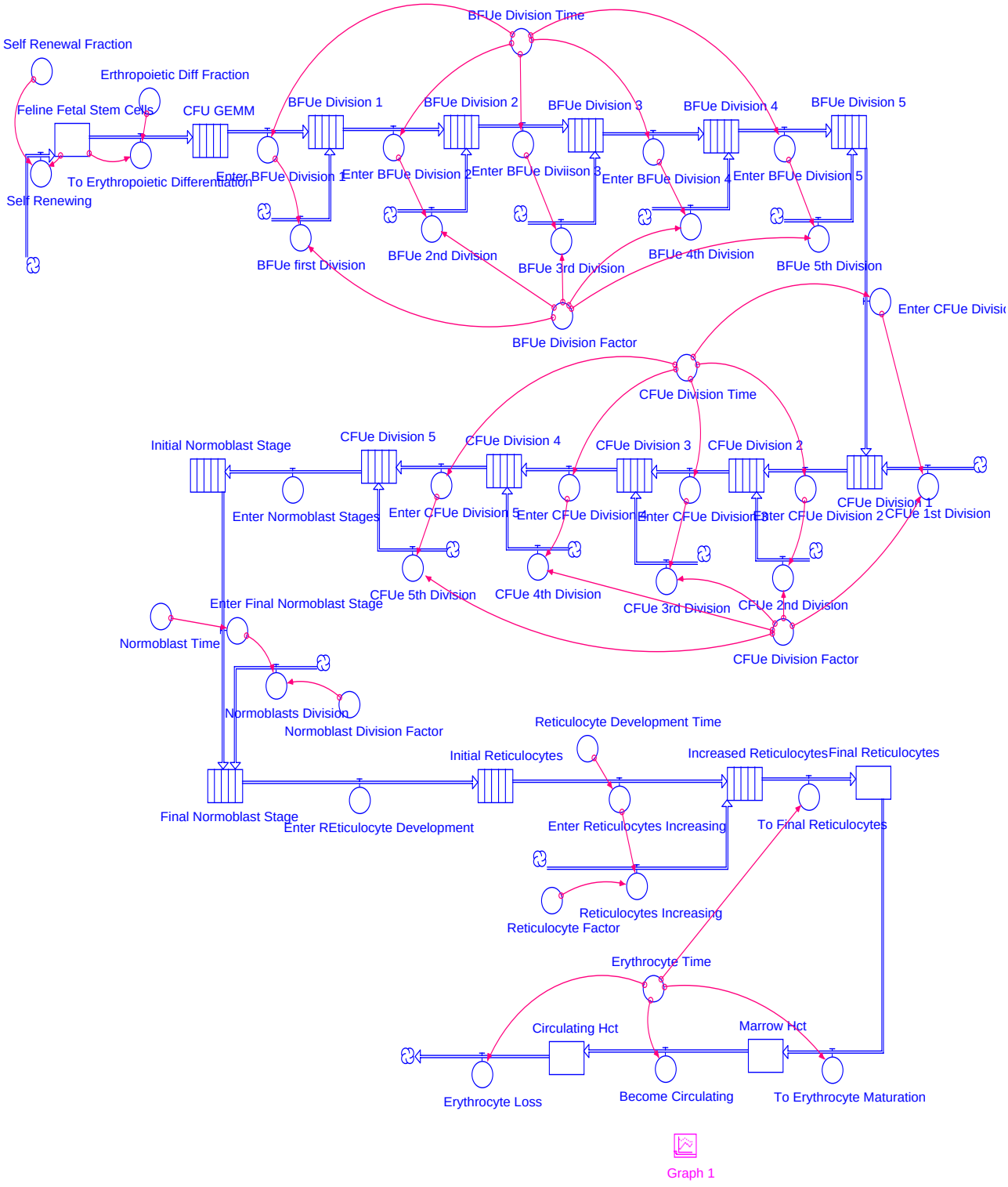
BFUe Division Time
Self Renewal Fraction
Erthropoietic Diff Fraction
Feline Fetal Stem Cells
CFU GEMM
BFUe Division 1
BFUe Division 2
BFUe Division 3
BFUe Division 4
BFUe Division 5
To Erythropoietic Differentiation
Self Renewing
Enter BFUe Division 1
Enter BFUe Division 2
Enter BFUe Diviison 3
Enter BFUe Division 4
Enter BFUe Division 5
BFUe first Division
BFUe 2nd Division
BFUe 3rd Division
BFUe 4th Division
BFUe 5th Division
BFUe Division Factor
Enter CFUe Divisi
CFUe Division Time
Initial Normoblast Stage
CFUe Division 5
CFUe Division 4
CFUe Division 3
CFUe Division 2
CFUe Division 1
Enter Normoblast Stages
Enter CFUe Division 5
Enter CFUe Division 4
Enter CFUe Division 3
Enter CFUe Division 2
CFUe 1st Division
CFUe 5th Division
CFUe 4th Division
CFUe 3rd Division
CFUe 2nd Division
Enter Final Normoblast Stage
Normoblast Time
CFUe Division Factor
Normoblasts Division
Normoblast Division Factor
Reticulocyte Development Time
Initial Reticulocytes
Increased Reticulocytes
Final Reticulocytes
Final Normoblast Stage
Enter REticulocyte Development
Enter Reticulocytes Increasing
To Final Reticulocytes
Reticulocytes Increasing
Reticulocyte Factor
Erythrocyte Time
Circulating Hct
Marrow Hct
Erythrocyte Loss
Become Circulating
To Erythrocyte Maturation
Graph 1

Figure 2. The Mathematical Model of Normal Feline Erythropoiesis. On the model layer, the elements described above were used in the construction of normal feline erythropoiesis.

Mathematical Modeling of FeLV-KT-infected Feline Erythropoiesis

Specific Aims

It is believed that FeLV-KT targets the fifth mitotic stage of development of the BFU-E cells, due to the presence of a particular protein on the cell surface at this stage. It is the aim to introduce the virus at this stage in the model, with everything else resembling normal feline erythropoiesis, in order to display a characteristic decline in red blood cells within the model, which is also seen in experimentally infected cats. The model was constructed for the comparison to real-system outputs, in the hopes that it could be expanded to predict other erythro- and lymphopoietic disruptions and outcomes.

Rationale

Once EA is induced by the abatement of precursor cells in the 5^{th} mitotic BFU-E stage by the targeted attack of FeLV-KT, hematocrit (Hct) decreases in a characteristic manner. To show that this effect is reproducible and is due to the targeted infection of a particular cell population, the normal erythropoietic pathway will be disrupted by the introduction of the virus into the model at this point. The amount of viral particles represented will be the average number of focus forming units (ffu) inoculated into experimental animals.

Method

Bench top research was conducted by Dr. E. A. Hoover at Colorado State University. The real system outputs from the following experiments were used as a comparison to modeling outputs and a basis for the construction of the model.

Cats

Cats used were derived exclusively from a nonseasonal SPF breeding colony originated in the Department of Veterinary Pathobiology, The Ohio Sate University and re-established in the Department of Veterinary Pathology, Colorado State University. These cats were free of FeLV exposure. Fifty-six juvenile SPF cats (mean age 72.2 +/- 1.6 days) were inoculated with the Kawakami Theilen strain of FeLV (FeLV-KT). Twenty-seven littermates or age-matched SPF cats served as controls.

Virus Inoculation and Sampling

FeLV-KT was employed as an infectious spleen homogenate derived from serial passage of virulent virus in SPF cats.[4, 13-14] Juvenile cats were inoculated intraperitoneally with between 1.3×10^3 and 2.3×10^5 focus forming units (ffu) of FeLV-KT (mean ffu, 7.0×10^4 +/- 1.0×10^4). Both FeLV-inoculated and control cats received 10 mg/kg of methyl prednisolone acetate (MPA) intramuscularly at the time of and 7 days post inoculation (DPI). At 7 day intervals after the original inoculation, both control and inoculated cats were anesthetized with ketamine hydrochloride and 2.5 ml blood was collected for the following determinations: total and differential cell count, reticulocyte count, erythrocyte packed cell volume, FeLV p27 antigen in leukocyte, and antibody against the feline oncornavirus-associated cell membrane

antigen (FOCMA) and antibody against FeLV. Heparinized femoral or humoral bone marrow aspirates (1ml) from 6 inoculated and 6 control cats were collected for in vitro assay of CFU-E/BFU-E and bone marrow cytology.

Cats were euthanized when the VPRC was less than 5%. Post mortem examination was performed on all cats and duplicate tissues were fixed in phosphate-buffered formalin and absolute methanol for histopathology and for identification of FeLV p27 antigen distribution respectively.

Infectious FeLV Quantitation

Sera and homogenates of spleen and bone marrow from FeLV infected and control cats were examined for infective FeLV with the clone 81 focus induction assay described by Fischinger et al.[15]

Latent FeLV Detection

Latent FeLV in bone marrow cells was reactivated by culture of 5×10^7 bone marrow mononuclear cells in 25 cm^3 flasks for 7 days.[16] Supernatants were assayed for infectious virus as described above.

In Vitro CFU-E/BFU-E Determination

Marrow mononuclear cells were separated by colloidal silica buoyant density centrifugation (density 1.070 g/ml) and cultured as described by Abkowitz et al.[17] Erythropoietic, purified from the plasma of anemic sheep (Connaught, Willowdale, Ontario, Canada) was added to the cultures (0.5 units/ml); no conditioned media were

used. Colonies were enumerated in duplicate cultures by inverted plate phase contrast microscopy; CFU-E were counted on day 5 and BFU-E on day 11 of culture.

Mathematical Modeling

By interrupting the model of normal erythropoiesis at the 5th mitotic BFU-E stage through the introduction of an element representing FeLV-KT, a characteristic loss of Hct should develop and lead to a similar slope of the graph shown by real system outputs.

It has been proposed that end stage aplastic anemia occurs as a secondary effect to the decline of the erythroid compartment.[18] By using Stella 5.1.1 to create a model of FeLV-KT-infected erythropoiesis, we demonstrate how simulated cytopathicity, at the level of the BFU-E, displays the same kinetics of the anemia observed in cats with experimentally induced FeLV-erythroid aplasia. The simulated decline in BFU-E creates an impediment to further maturation and differentiation of committed stem cells entering this pathway. Cessation of red cell production and an increase of stem cells committed to the erythropoietic pathway in an attempt to relieve the loss of red cells are two results of this impediment. As red cells are lost and no further cells become available, through viral targeting of the BFU-E, the body's demand increases and a shift occurs away from the production of other blood cell types. This shift from the production of other hematopoietic cell lineages is an attempt by the HSC to fulfill the body's erythropoietic demand. The greater the loss of red cells the higher the number of HSC committed to the erythropoietic differentiation pathway.

Ablation of BFU-E proliferation antecedent to all other hematologic changes indicates that the BFU-E progenitor cell is the most important target cell for the cytopathic effect of anemogenic FeLV-KT. Our findings confirm those of Onions and Testa who have reported that FeLV-KT, or FeLV subgroup C, suppresses BFU-E in experimentally infected newborn kittens.[19] Using virulent in vivo selected, highly anemogenic FeLV isolates, BFU-E abatement is virtually concurrent with retroviral infection of hematopoietic cells. When this data was used in construction of a mathematical model, it supported the experimental results of the effect of FeLV-KT upon the BFU-E, demonstrating that subsequent marrow failure is a secondary outcome to the loss of BFU-E progenitors

Data from original experiments, carried out by Dr. E.A. Hoover and Dr. Peter Gasper at The Ohio State University and Colorado State University, were entered into the software program Excel. Cats used to obtain this data were derived exclusively from a nonseasonal SPF breeding colony originated in the Department of Veterinary Pathobiology, The Ohio State University and re-established in the Department of Pathology, Colorado State University in 1981.[20] These cats were free of FeLV exposure. Fifty-six juvenile SPF cats (mean age 72.2 +/- 1.6 days) were inoculated with FeLV-KT. Thirty of these cats exhibited FeLV-associated EA. Twenty-seven littermate or age-matched SPF cats served as controls. FeLV-KT was employed as an infectious spleen homogenate derived from serial passage of virulent virus in SPF cats.[20] Juvenile cats were inoculated intraperitoneally with between 1.3×10^3 and 2.3

x 10^5 focus forming units (ffu) of FeLV-KT. Both FeLV-inoculated and control cats received 1-mg/Kg of methylprednisolone acetate (MPA) intramuscularly at the time of and 7 days post inoculation (DPI). At 7 day intervals after inoculation, both control and inoculation cats were anesthetized with ketamine hydrochloride and 2.5 ml blood was collected for the following determinations: total and differential cell counts, reticulocyte count, erythrocyte packed cell volume (VPRC or Hct), FeLV-p27 antigen in leukocytes, antibody against the feline oncornavirus-associated cell membrane antigen (FOCMA) and antibody against FeLV. FOCMA is a protein expressed on certain feline cancer cells, especially lymphoma and leukemia cells. The presence of FOCMA antibodies in healthy cats often indicates a latent infection with FeLV. FeLV-p27 is a structural component of the FeLV inner viral core. This protein can be found in great abundance in infected blood cells and in soluble form in plasma and serum of viremic cats.

Heparinized femoral or humoral bone marrow aspirates (1 ml) from 6 inoculated and 6 control cats were collected for in vitro assay of Colony Forming Unit-Erythroid (CFU-E)/BFU-E and bone marrow cytology. Cats were euthanized when the VPRC was less than 5%. Post mortem examination was performed on all cats and duplicate sets of tissues were fixed in phosphate-buffered formalin and absolute methanol for histopathology and for identification of FeLV p27 antigen distribution, respectively. Data obtained and entered were from felines displaying FeLV infection with aplastic anemia, those latently infected and those used as controls. The information entered included results of the cell counts of BFU-E, CFU-E, reticulocytes, VPRC, or Hct,

lymphocytes, granulocytes, monocytes, the age of the cats, the weights of cats, antigen-antibody studies (FeLV and FOCMA) spanning a 140 day time period. The primary cell counts used in construction of the FeLV-KT-infected model were the BFU-E.

As mentioned above, in constructing the erythropoietic mathematical models the third tool employed was the converter. The converter appeared as a stand-alone circle on the Model Layer. This instrument served a utilitarian role in the software. It held values for constants, defined external inputs to the model, calculated algebraic relationships and served as the repository for graphical functions. In general, it converted inputs into outputs. Within the structure of our model of erythropoiesis, it served several different functions. We put it into play to control division time, death, division, differentiation and maturation factors, total cell numbers and, most importantly, it represented the feline leukemia virus.

In our model, we "transplanted" 8 HSC into the system. This number was chosen as it has been shown that only 8 HSC are required to give rise to the complete hematopoietic architecture after total body irradiation (TBI).[18] The pathway was modeled in log scale analog. Both the BFU-E and the CFU-E cell compartments contained 5 distinct mitoses. The virus was introduced using a converter entitled "Introduction of FeLV". The mean focus forming units (ffu) of viral particles was written within this converter and we employed the average amount of the real system

inoculation, 7 x 10^4 ffu. Additionally, FeLV was created within the model to mimic normal viral reproduction and death. The loss of BFU-E was initiated at the fifth stage of division, using a flow to represent BFU-E loss. This loss only occurred when a toggle switch, to which the virus was connected, was turned on. The software contained these "switches" in order to permit model builders to create on/off behavior for variables or sectors in a model. When attached to a converter, a switch would return a 1 when on and a 0 when off. An equation was written within the BFU-E loss flow regulator allowing the infection to occur at this fifth stage of division when the toggle was "on" through the interaction of a connector from the "Introduction of FeLV" to the BFU-E loss flow. The reasons for setting the loss at the fifth mitotic stage of BFU-E development are two-fold: (1) we suspected that certain cell surface proteins, with which the virus interacts, were either not accessible or not expressed prior to reaching this stage of development. Since our initial hypothesis it has been shown that the FeLV-C receptor, named FELVCR or gp70, does not appear on the surface of BFU-E cells until the fifth division stage.(2) Recent evidence by Abkowitz, et al., has shown that the virus interacts and disrupts the BFU-E at this 5^{th} division stage or, possibly, between BFU-E division stage 5 and CFU-E division stage 1.[21] Other connectors were used to initiate the effects of the viral infection at the level of the reticulocytes, marrow erythrocytes and circulating erythrocytes. The equations used to simulate virus interaction and subsequent effects are as follows:

(1) Within the BFU-E loss flow the equation stated "IF Introduction_of_FeLV=1 THEN BFUe Death ELSE 0". As may be obvious, this instructed the flow to lose

BFU-E cells only upon introduction of the virus, that is, when the toggle switch returned a value of 1.

(2) When the Introduction of FeLV toggle returned a value of 1 a connector initiated a difference in the time value within the Final Reticulocytes, Marrow Erythrocytes and Circulating Erythrocytes compartments. No other direct changes or viral effects were placed upon these compartments via this connection.

The expression shown in (1) enabled the toggle switch to control the presence and absence of FeLV, and, subsequently, the infection of the BFU-E cells. This infection further impacted all cell compartments along the erythropoietic differentiation pathway by merely placing the virus action at this location. As stated earlier, the virus either infected the BFU-E cells (toggle switch returned a value of 1 and was turned on; virus was present), stopping further division and simulating cell death or was absent from the cells (toggle switch returned a value of 0 and was turned off). The loss of BFU-E cells and slope of the decline in Hct, as well as the shift of HSCs to the erythropoietic pathway, were then analyzed through the software's graphical and animation utilities.

As mentioned previously, one of the major benefits of using this particular data-analysis software tool was the automatic assignment of differential equations to each part of the model. In calculus parlance, the flows represented time derivatives; stocks were the integrals (or accumulations) of flows over time; converters contained micro-

logic of flows. Having such a software tool at our disposal allowed us to concentrate on the overall and more important aspects of building the model.

Once the model had been developed it was further tested by utilizing specific model validation equations. These equations will allow the demonstration of the amount of error found in the model and the comparison of the model BFU-E loss slope and Hct slope to that calculated from real system outputs.

Results

Responses to FeLV-KT Inoculation

Of the 56 juvenile cats inoculated with FeLV-KT, 100% (56/56) became persistently viremic. Eighty-three percent (47/56) were viremic by 14 DPI, 96% (54/56) by 21 DPI and 100% (56/56) by 35 DPI. Four FeLV-KT-positive cats died prior to any hematologic changes (one each at 17 and 19 DPI and two at 20 DPI) and exhibited thymic atrophy, diarrhea and generalized emaciation.

Three responses to FeLV-KT infection were observed. The majority of cats, 73%, (30/41) expressed acute FeLV-AA (VPRC <10% within 63 DPI), 22% (9/41) developed a protracted form of FeLV-AA (VPRC <10% in 70 to 170 DPI) and 5% (2/41) developed regressive infection with no hematologic changes and in which latent FeLV was reactivated by in vitro culture of marrow cells. Cats that developed either a protracted FeLV-AA or regressive latent infection were significantly older, larger and produced higher titers of FOCMA antibody when compared with cats with

acute FeLV-AA (Table 1; Fig. 3). Cats with protracted FeLV-AA had a significantly delayed onset of viremia, whereas cats with latent infection received significantly less infectious virus compared with cats with acute FeLV-AA (Table 1). FeLV and FOCMA antibody titers were significantly higher in cats with either the acute or the protracted response to FeLV-KT (Fig. 3; Fig. 4).

TABLE 1. Comparison of Cats Displaying Acute, Protracted and Latent FeLV-AA.

	AGE AT INOCULATION Days +/- SEM	**WEIGHT AT INOCULATION** gm +/- SEM	**INOCULUM TITER** 81 cell ffu +/- SEM	**ONSET OF VIREMIA** days post inoculation
Acute FeLV-AA* (n=30)	69.80 +/- 2.3[a,d]	807.23 +/- 47.8[a,b]	9.4×10^4 +/- 1.5×10^d	15.62 +/- 0.59[c]
Protracted FeLV-AA** (n=9)	78.22 +/- 4.6[a]	997.11 +/- 117.4[a]	8.8×10^4 +/- 3.2×10^4	18.67 +/- 3.1[c]
Latent FeLV*** (n=2)	83.5 +/- 9.5[d]	1264.50 +/- 184.5[b]	1.5×10^3 +/- 0^d	17.5 +/- 3.5

* VPRC <10% within 63 days post inoculation (DPI)
** VPRC <10% in 70 to 170 DPI
*** Regressive viremia with no significant hematologic changes

a P<0.05 comparing acute vs. protracted groups b P<0.05 comparing acute vs. latent groups

c P<0.1 comparing acute vs. protracted groups d P<0.1 comparing acute vs. latent groups

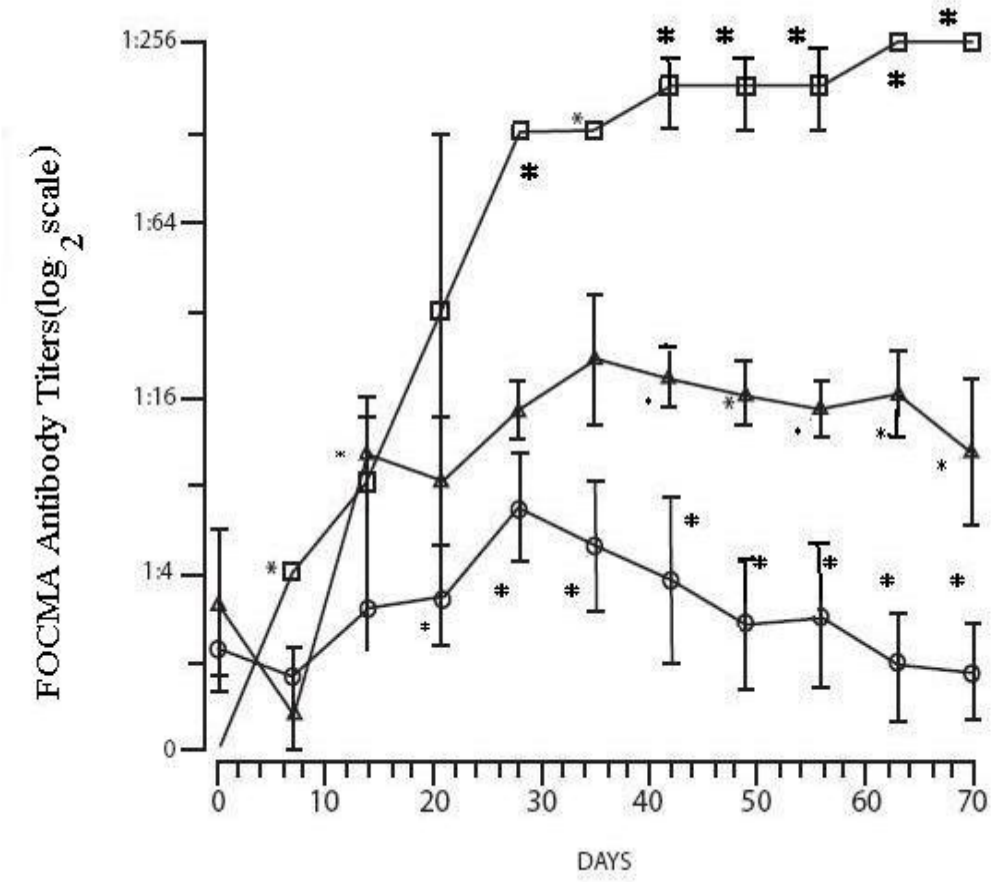

FIGURE 3. Determination of FOCMA antibody titers in cells of FeLV-KT-infected cats. At day 7 DPI and at 7 day intervals thereafter, FeLV-KT-infected cats were anesthetized with ketamine hydrochloride and 2.5 ml of blood was collected from each. Blood was incubated with antibodies against the feline oncornavirus-associated membrane antigen, which is known to present high titers in cats infected with FeLV and is frequently used as a determinant in cats that are FeLV-negative as a test for latent FeLV infection. Cats with acute FeLV have much higher FOCMA titers than those that are latently infected.

◯ = Acute FeLV-AA □ = Latent FeLV △ = Protracted FeLV-AA

* = $P<0.05$, * = $P<0.01$, Student t, Ho: $\mu_{Latent} = \mu_{Protracted}$

* = $P<0.05$, * = $P<0.01$, Student t, Ho: $\mu_{Protracted} = \mu_{Acute}$

* = $P<0.05$, * = $P<0.01$, Student t, Ho: $\mu_{Acute} = \mu_{Latent}$

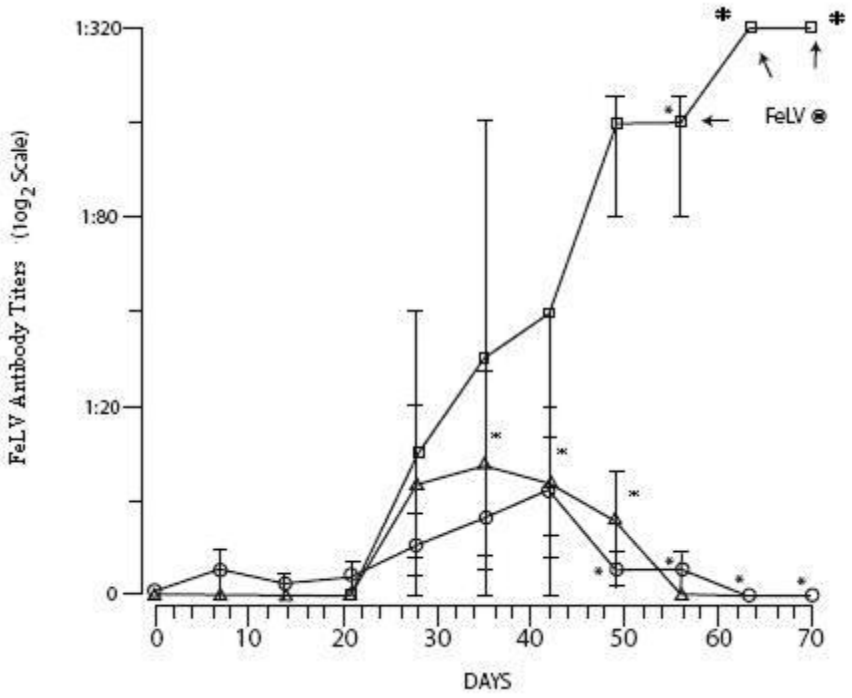

FIGURE 4. Determination of FeLV antibody titers in FeLV-KT-infected cats. At 7 day intervals, FeLV-infected cats were anesthetized with ketamine hydrochloride and 2.5 ml of blood was obtained from each. Antibody against FeLV was used to determine the titer of FeLV in infected cats. Further, spleen and bone marrow homogenates were examined for infective FeLV using the clone 81 focus induction assay (data not shown).[15]

◯ = Acute FeLV-AA □ = Latent FeLV △ = Protracted FeLV-AA

* = $P<0.05$, ** = $P<0.01$, Student t, Ho: $\mu_{Latent} = \mu_{Protracted}$

* = $P<0.01$, Student t, Ho: $\mu_{Protracted} = \mu_{Latent}$

* = $P<0.05$, Student t, Ho: $\mu_{Acute} = \mu_{Latent}$

Hematologic Changes

Hematologic features of FeLV-KT-induced aplasia were identical in cats with either acute or protracted FeLV-AA. Protracted FeLV-AA was distinguished from acute FeLV-AA by a longer interval between the onset of viremia and the onset of aplasia.

Once anemia commenced, the rate of VPRC decline in both groups were similar (Fig. 5; Fig. 6). Reticulocytes, granulocytes, monocytes and lymphocytes also were suppressed in cats with acute FeLV-AA as compared with controls beginning 21 or 28 DPI (Fig. 6; Fig. 7; Fig. 8; Fig. 9).

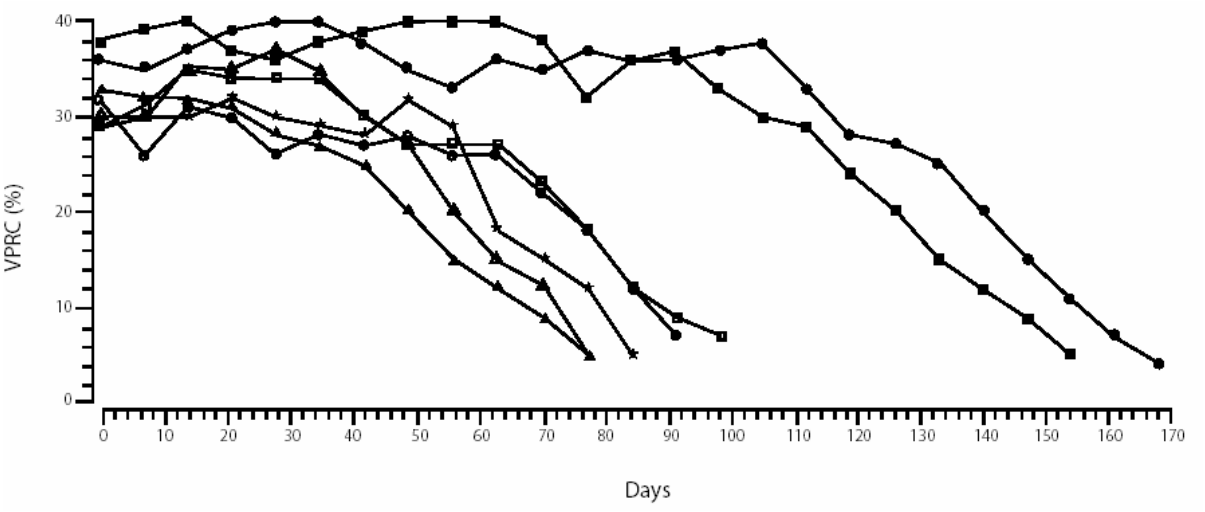

FIGURE 5. Determination of the erythrocyte packed cell volume (VPRC or Hct) in FeLV-KT-infected cats. Responses of erythrocytes in cats infected with FeLV-KT are demonstrated in the graph. Blood samples, collected from anesthetized cats at 7 day intervals, were centrifuged and the red cell volume was compared with the total blood count and expressed as a percent. The graph shows cats with both acute FeLV-AA and protracted FeLV-AA. Protracted FeLV-AA is displayed as the two slopes to the far right.

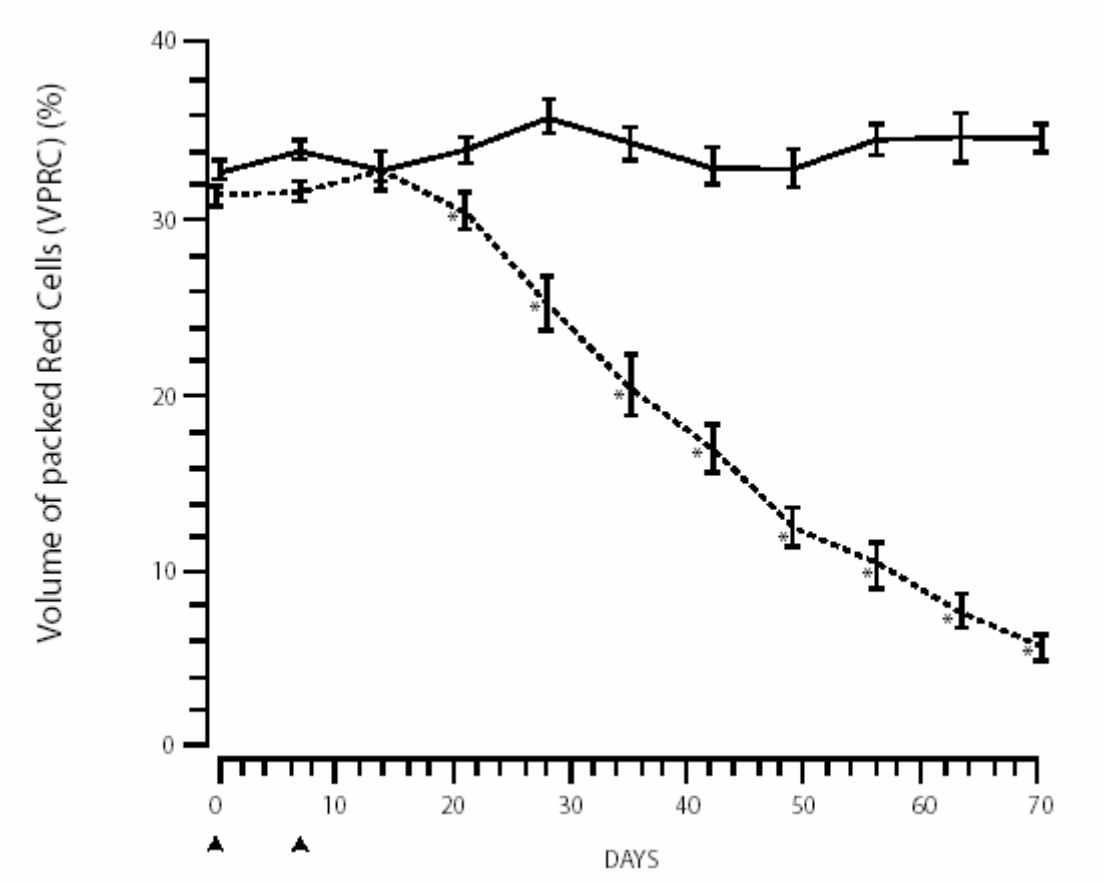

FIGURE 6. Comparison of the volume of packed red cells from cats displaying FeLV-KT infection and control littermates, which were non-infected. Data were obtained at 7 day intervals from infected cats and littermate control cats by determining the VPRC or Hct percent, as in Figure 5. Averages were calculated from cats displaying FeLV infection and control cats. One mg/Kg of Methyl prednisolone acetate was injected into each cat in both control and infected cat groups, as shown by the dark triangle. MPA was used to suppress effects of the immune system in order to determine the true percent of VPRC.

* = $P<0.01$ Ho: $\mu_{Control} = \mu_{FeLV\text{-}AA}$

—— = Controls, ---- = FeLV-KT inoculated, ▲ = MPA

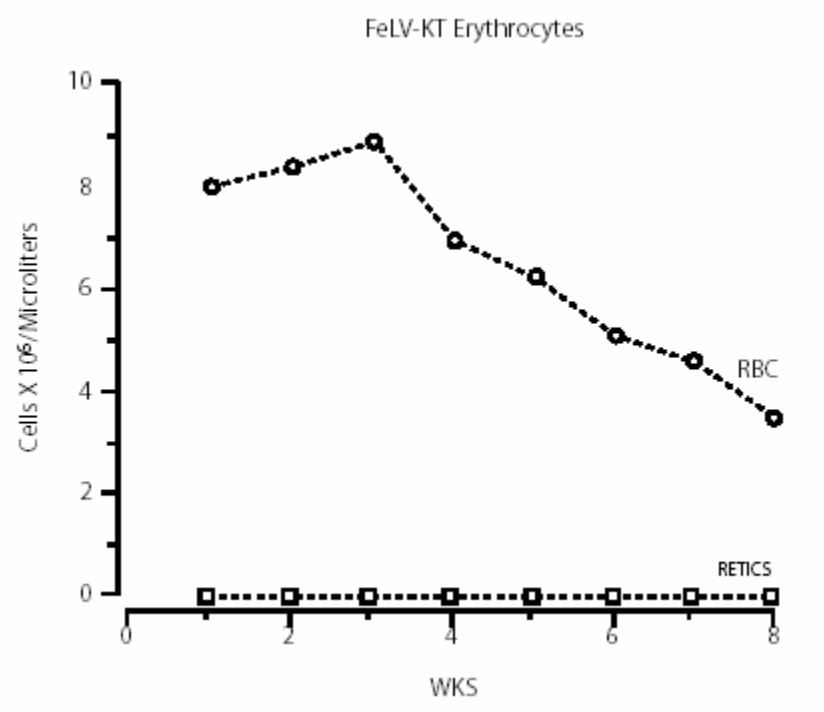

FIGURE 7. The comparison of red blood cell counts and reticulocyte counts in cats displaying acute FeLV-KT infection. Beginning at week one, continuing through week 8, RBC and reticulocyte cell counts were accomplished from circulating blood in cats with acute FeLV-KT infection. Averages are shown from all cats that displayed acute FeLV-KT infection.

◘ = Reticulocytes; ○ = RBCs

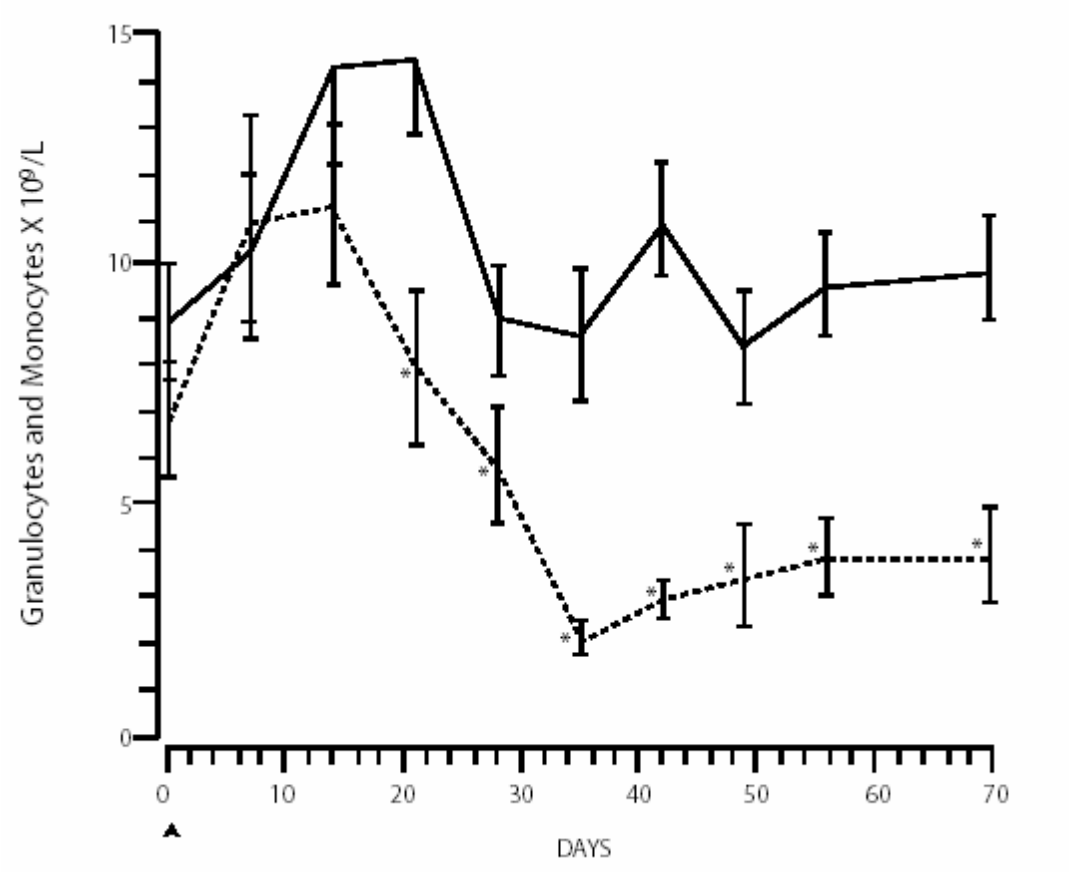

FIGURE 8. Differential cell count (Diff) showing the Granulocyte/Monocyte counts of white blood cells in acute FeLV-KT-infected cats compared to littermate control cats. At 7 day intervals, control and FeLV-KT-infected cats were anesthetized with ketamine hydrochloride and 2.5 ml of blood was obtained. At the time of inoculation (day 0) cats received 1 mg/Kg of MPA, shown as the dark triangle in the figure. Control cats also received the same amount of MPA. The graph of lymphocytes from the differential cell counts is shown on the following page. Granulocytes are often named polymorphonuclear leukocytes and include neutrophils, eosinophils and basophils. Although not a primary target for FeLV-KT, the lower cell counts seen in FeLV-KT infected cats most likely corresponds to the shift of pluripotential stem cells to the erythropoietic pathway in an attempt to alleviate the loss of erythrocytes. Additionally, the lowered counts in both FeLV-KT-infected and control cats are expected when MPA if given.

* = $P<0.01$, Student t, Ho: $\mu_{Control} = \mu_{FeLV\text{-}AA}$

—— = Controls, ----- = FeLV-KT inoculated, ▲ = MPA

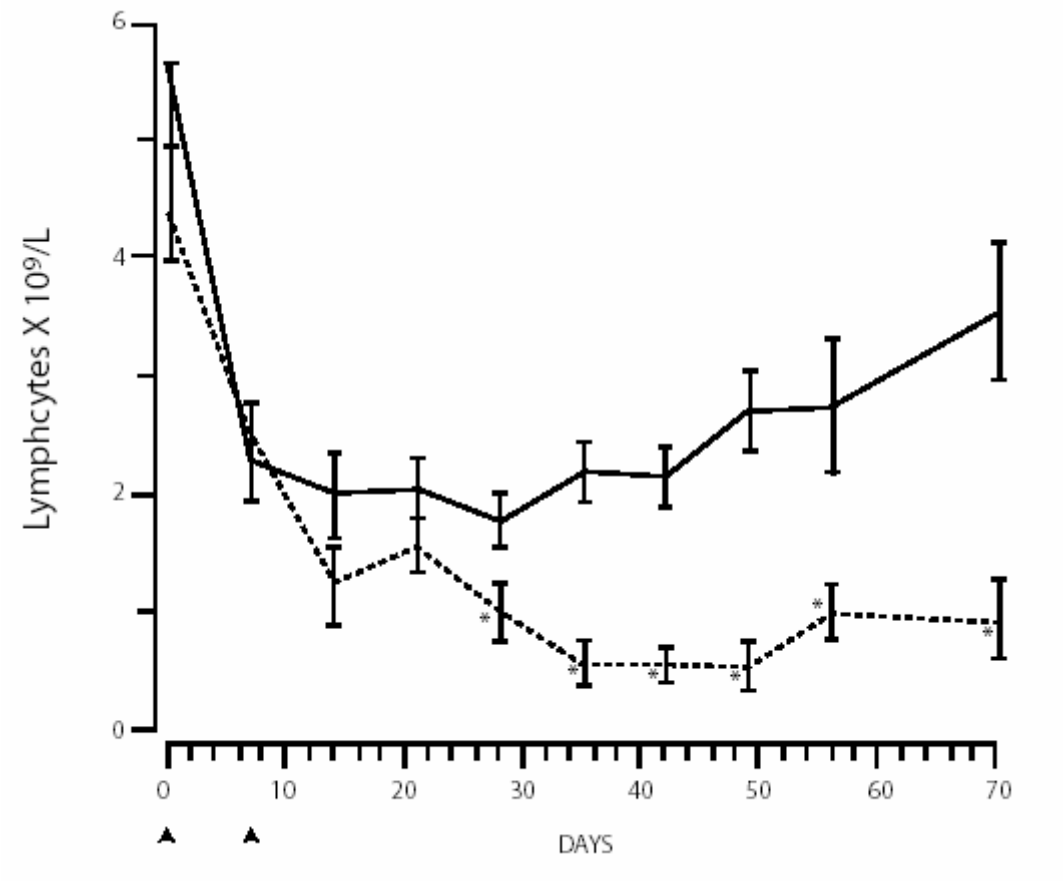

FIGURE 9. Results of the lymphocyte cell counts from the differential cell counts of FeLV-KT inoculated cats compared to control littermate cats. At 7 day intervals after inoculation with FeLV-KT, both control and inoculation cats were anesthetized with ketamine hydrochloride and 2.5 ml of blood was collected. Both FeLV-inoculated cats and control cats received 1 mg/Kg of MPA at the time of inoculation and 7 DPI. Some suppression of lymphocytes is naturally observed due to these injections. The lower lymphocyte counts displayed in FeLV-KT-infected cats is, again, most likely due to the assumption that pluripotant stem cells have shifted to the attempt to relieve the loss of erythrocytes.

* = $P<0.01$, Student t, Ho: $\mu_{Control} = \mu_{FeLV\text{-}AA}$

—— = Controls, ----- = FeLV-KT inoculated, ▲ = MPA

Hematopoietic Changes

Abatement of marrow BFU-E was the earliest detected event in the evolution of FeLV-AA. A mean 19% in marrow BFU-E of inoculated cats as compared with controls was present at 14 DPI (Fig. 10). FeLV p27 antigen was detected in circulating leukocytes and thrombocytes in 93% of the inoculated cats at that time. By 19 DPI, mean BFU-E and CFU-E were reduced by 38% and 31% respectively. At 28 DPI, when a significant decline in VPRC was first evident, BFU-E and CFU-E were reduced to 20% of control values (Fig. 10).

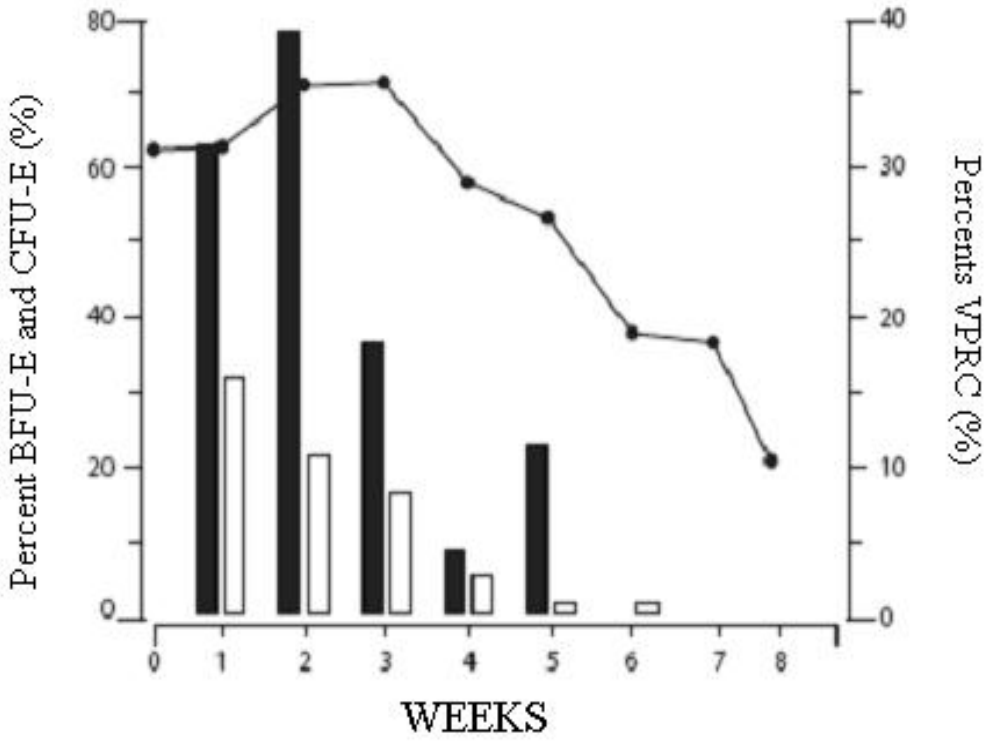

FIGURE 10. The determination of erythroid progenitor cell growth in acute FeLV-KT-infected cats, compared to VPRC. One ml of heparinized femoral or humoral bone marrow aspirates from 6 inoculated cats were collected for in vitro assay of colony forming units – erythroid and burst forming units – erythroid. Marrow mononuclear cells were separated by colloidal silica buoyant density centrifugation (density 1.070 g/ml) and cultured. Erythropoietic® purified from the plasma of anemic sheep (Connaught, Willowdale, Ontario, Canada) was added to the cultures (0.5 units/ml). Colonies were enumerated in duplicate cultures by inverted phase contrast microscopy; CFU-E were counted on day 5 and BFU-E on day 11 of culture. The results were then compared to the VPRC. The averages from all cats displaying acute FeLV-KT is shown as a percent.

□ = Colony Forming Units - erythroid, CFU-e

■ = Burst Forming Units – erythroid, BFU-e

▬ = VPRC

Pathologic Changes

Lesions were restricted to lymphoid and hematopoietic tissues. Histologic findings in marrow of aplastic cats (VPRC <10%) were marked pancytopenia with apparent megakaryocytic hyperplasia as compared with controls (Fig. 11). Other lesions were generalized pallor, thymic atrophy and pannodal lymphoid depletion (VPRC <10%). Consistent with the rapid depletion of lymphohematopoietic cells produced by FeLV-KT was the absence of weight loss in cats with acute FeLV-AA as compared with controls (Fig. 12).

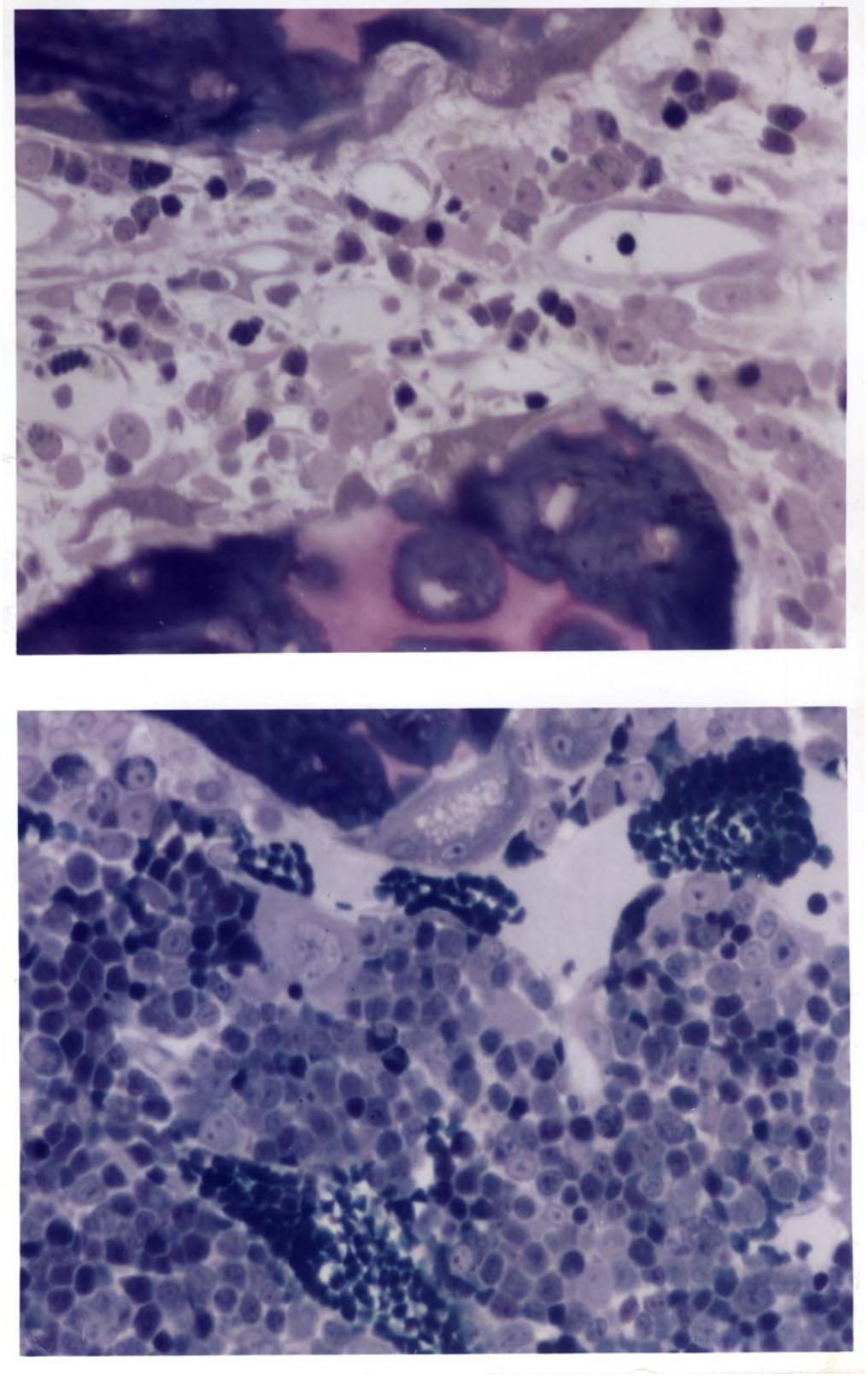

a.

b.

FIGURE 11. Bone marrow histology of FeLV-KT-infected cats compared to control littermate cats. Cats were euthanized when the VPRC was less than 10%. Post mortem examinations were performed on all cats and duplicate tissues were fixed in phosphate-buffered formalin and absolute methanol for histopathology. Histologic findings in the marrow of aplastic cats (VPRC < 10%) were marked pancytopenia with apparent megakaryocytic hyperplasia as compared with controls.

a. = Metaphyseal Bone Marrow from Normal Juvenile Cat.
b. = Metaphyseal Bone Marrow From Littermate Cat with FeLV-AA.

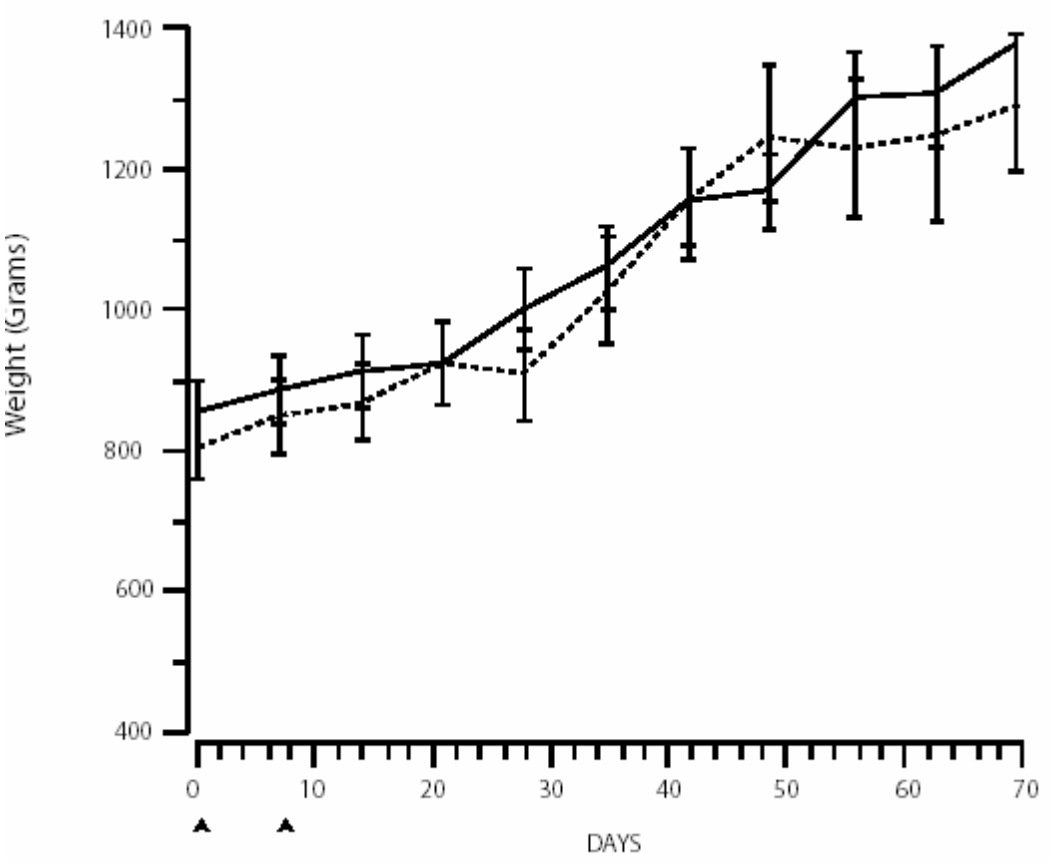

FIGURE 12. Comparison of body weights of FeLV-KT-infected cats with non-infected, control littermates. Weights of both inoculated and control cats were obtained after there were anesthetized with ketamine hydrochloride at inoculation and at 7 day intervals, thereafter. MPA was given at the time of inoculation and at 7 DPI. The absence of weight loss in cats with FeLV-AA was consistent with the rapid depletion of lymphohematopoietic cells.

—— = Controls, ----- = FeLV-KT inoculated, ▲ = MPA

Mathematical Modeling of FeLV-KT-infected Erythropoiesis

Since FeLV-KT is specific at the level of the BFU-E, we placed the virus within this compartment in the model at the fifth mitotic stage (Figure 13). Our choice was motivated by factors previously outlined. Further, it requires time for the interaction of the virus with a cell surface receptor, subsequent cell internalization and mobilization of the virus to the nucleus and the consequential viral interruption of further BFU-E development.

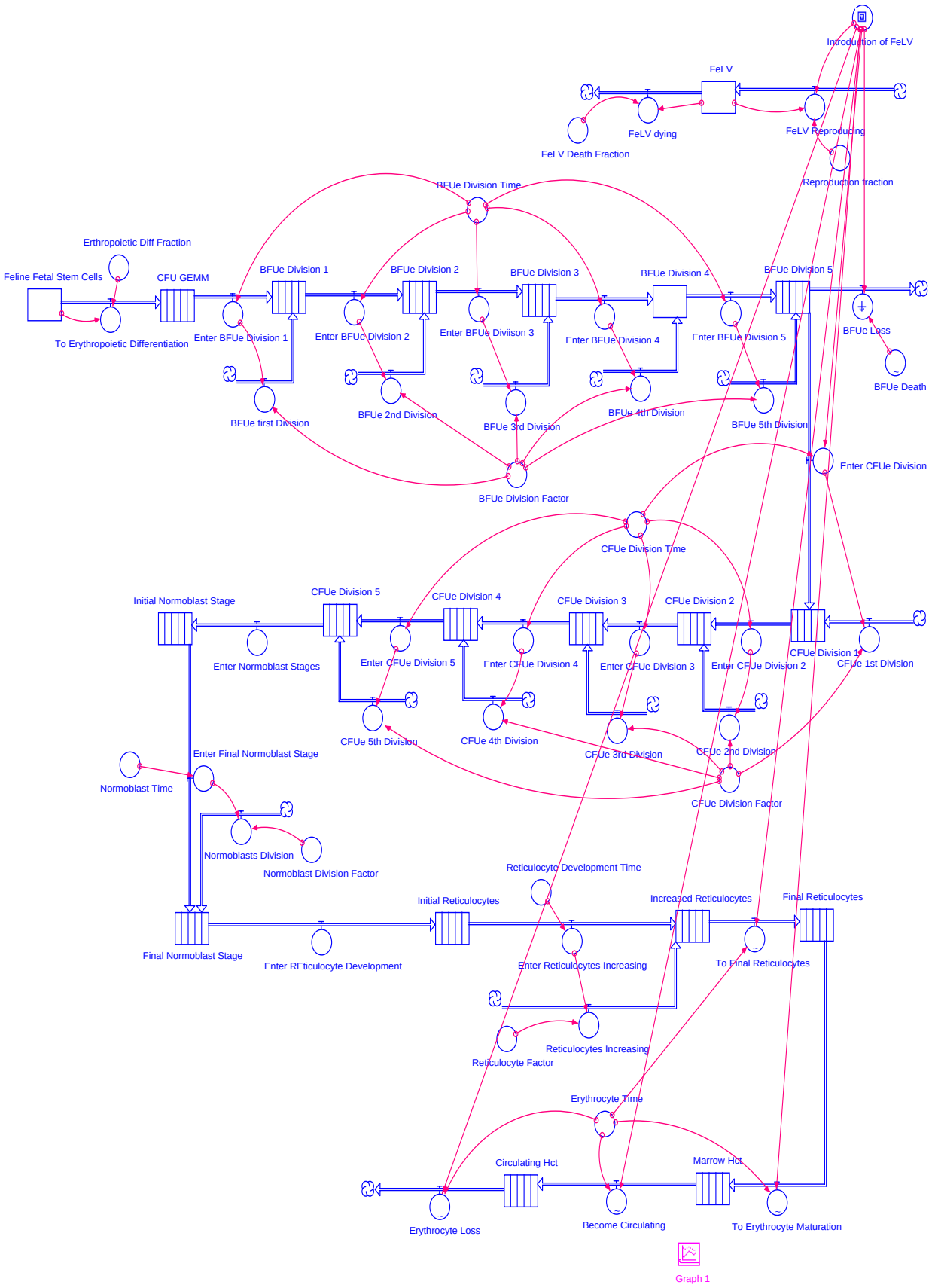
Introduction of FeLV
FeLV
FeLV dying
FeLV Reproducing
FeLV Death Fraction
Reproduction fraction
BFUe Division Time
Erthropoietic Diff Fraction
Feline Fetal Stem Cells
CFU GEMM
BFUe Division 1
BFUe Division 2
BFUe Division 3
BFUe Division 4
BFUe Division 5
BFUe Loss
BFUe Death
To Erythropoietic Differentiation
Enter BFUe Division 1
Enter BFUe Division 2
Enter BFUe Diviison 3
Enter BFUe Division 4
Enter BFUe Division 5
BFUe first Division
BFUe 2nd Division
BFUe 3rd Division
BFUe 4th Division
BFUe 5th Division
BFUe Division Factor
Enter CFUe Division
CFUe Division Time
Initial Normoblast Stage
CFUe Division 5
CFUe Division 4
CFUe Division 3
CFUe Division 2
CFUe Division 1
CFUe 1st Division
Enter Normoblast Stages
Enter CFUe Division 5
Enter CFUe Division 4
Enter CFUe Division 3
Enter CFUe Division 2
CFUe 5th Division
CFUe 4th Division
CFUe 3rd Division
CFUe 2nd Division
CFUe Division Factor
Enter Final Normoblast Stage
Normoblast Time
Normoblasts Division
Normoblast Division Factor
Reticulocyte Development Time
Initial Reticulocytes
Increased Reticulocytes
Final Reticulocytes
Final Normoblast Stage
Enter REticulocyte Development
Enter Reticulocytes Increasing
To Final Reticulocytes
Reticulocytes Increasing
Reticulocyte Factor
Erythrocyte Time
Circulating Hct
Marrow Hct
Erythrocyte Loss
Become Circulating
To Erythrocyte Maturation
Graph 1

Figure 13. The Mathematical Model of FeLV-KT Infected Feline Erythropoiesis. The model was created to verify that viral infection at the 5th mitotic stage of BFU-E development creates a block, leading to death of cells at this stage and subsequent fatal erythroid aplasia. The death of these cells causes a loss of Hct in a characteristic decline that is graphically reproducible in both real-system outputs and outputs from the mathematical model.

However, when we placed the virus in the model to interact with the first through the fourth mitotic stages of BFU-E development this characteristic slope of Hct was not shown. In fact, when cells were infected at these stages fatal erythroid aplasia was not demonstrated. The slope of the graph of BFU-E loss at these different points would initially decline but quickly recover and maintain the "normal" cell count for that phase of cell development. The only explanation we have for this effect is due to the division factor and the division times at the stages past these points. These variables would remain stable and may have allowed the recovery of the mitotic stage interacting with the FeLV.

When the virus was present in the model, cells developing in the BFU-E stage were blocked from further erythropoietic expansion and differentiation and entered cell loss, or death. Data from the original experiments and logarithmic scale were incorporated into the computer model. By day 28, the model revealed a significant increase in BFU-E cell death (Fig 14). The model FeLV-KT-infected Hct appeared steeper than the graph of the actual feline Hct, graphed as a percentage of the total packed cell count. In actuality, the slope of the loss of marrow red cells and circulating red cells nearly matched the average slope calculated from graphs of Hct decline in laboratory animals (Fig 5, 15 and 16).

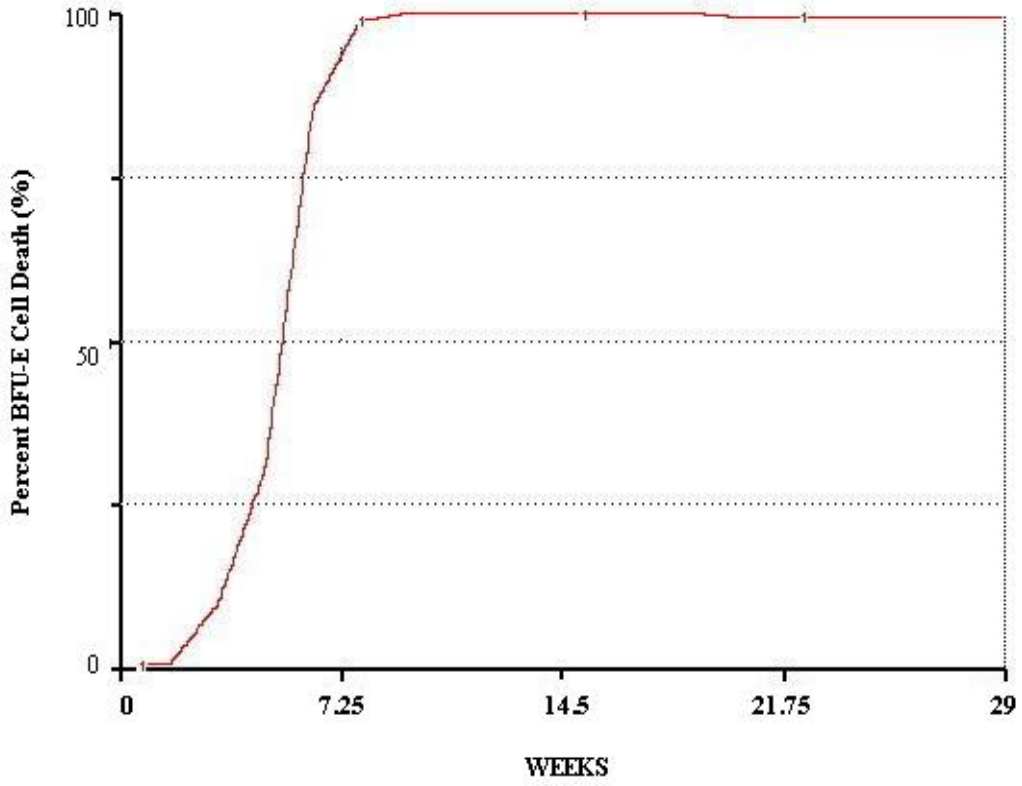

FIGURE 14. Mathematical modeling graph of the percent cell death of FeLV-KT-infected BFU-E. The graph displays the percent loss of BFU-E once FeLV-KT infection commences within the model. The graph shows the percent of BFU-E as they are lost after entering the fifth mitotic division stage and interacting with FeLV-KT. The model predicts a 50% decline in BFU-E around day 30 of the infection, with the complete loss of BFU-E by day 70.

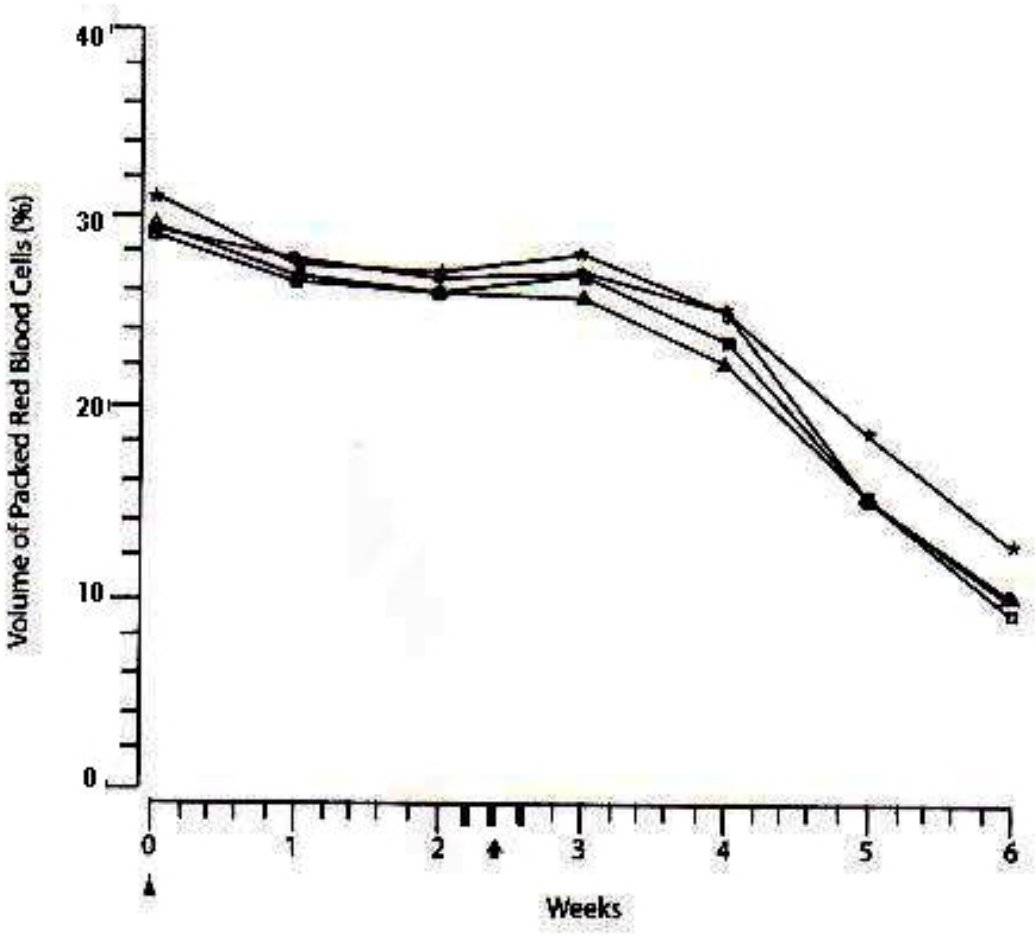

FIGURE 15. Graph of the decline of Hct in cats inoculated with FeLV-KT over time. At 7 day intervals, after the original inoculation, FeLV-KT-infected cats were anesthetized with ketamine hydrochloride and the percent of packed red bloods cells (VPRC) was examined. Latently FeLV-infected cats were analyzed after it was clear that active infection had commenced, as determined by FeLV antibody titers, differential cell counts, VPRC, BFU-E and CFU-E determination. Cats were euthanized when the VPRC or Hct was 5%. The arrow points to darkened markers, indicating the deaths of four cats. These cats died prior to becoming persistently viremic. One cat each died on day 17 and 19, while two cats expired on day 20. The average slope of the loss of Hct from all cats was 0.532.

▲ = MPA ↑ = cat deaths prior to persistent FeLV infection

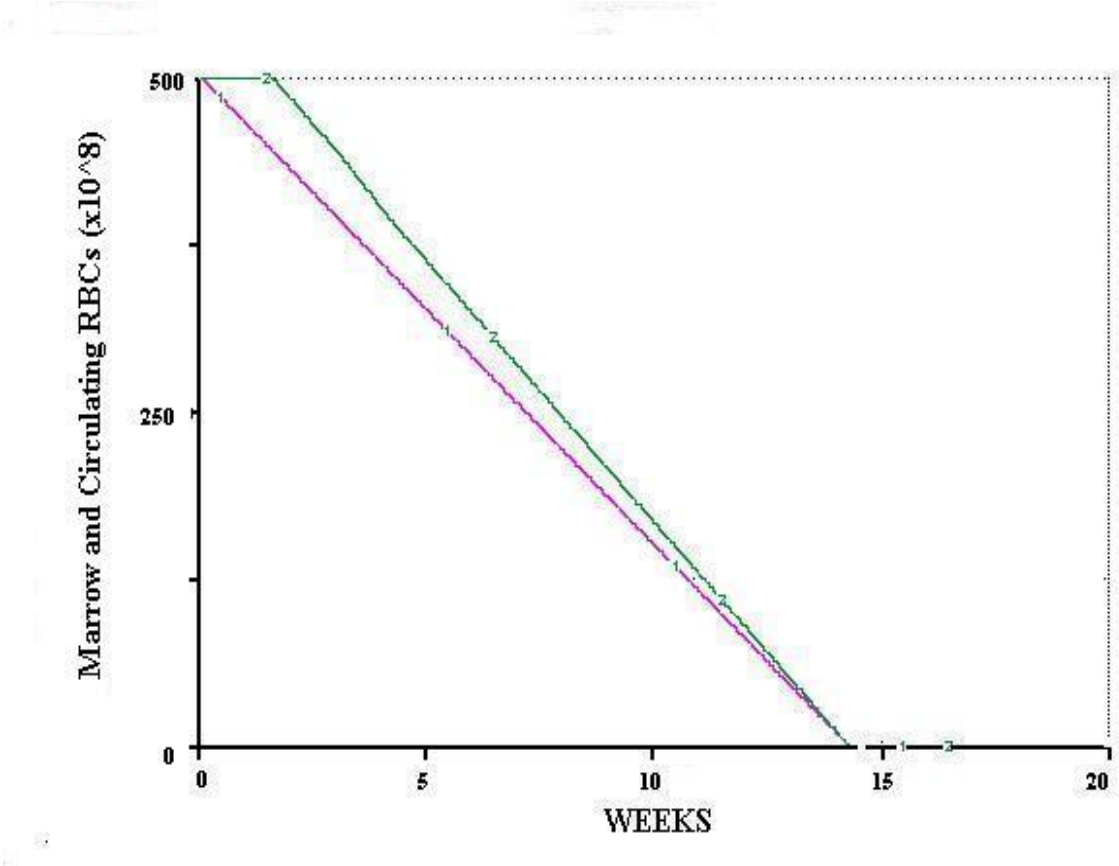

Figure 16. Results of FeLV Infection upon the Hct from the Mathematical Model. After FeLV interacted or "infected" the BFU-E cell compartment at the fifth mitotic stage of development, the Hct began an immediate decline. The pink line represents the marrow Hct, while the green displays the circulating Hct. Circulating Hct begins to decline shortly after Marrow Hct, as the Circulating Hct is dependent on its supply from the Marrow Hct. The slope of circulating Hct was 0.543 and the marrow Hct was 0.5.

We endeavored to embody a non-plastic system within a highly, synthetic environment. When a stem cell is committed to erythropoietic differentiation, the cell passes through 5 distinct mitoses within the BFU-E reservoir, as stated earlier. These take place every 8 hours. The generation time, on average, is around 24 hours, but can be reduced to 8 hours or prolonged to 27.[22] Usually, only 33% of the cells are in the

active cell cycle as compared to CFU-E, in which 100% of these cells are actively involved in cell cycling. [22] Within the CFU-E stage, the generation time equals the cell cycle time of 8 hours.[22] Thus a feline requires an average of 70 days to completely saturate the mature red blood cell compartment. Due to the reserve amount of reticulocytes and red blood cells (5×10^8), once aplasia begins, a total loss of RBCs should develop within 70 to 140 days. Our mathematical model agreed with this hypothesis and supported the evidence from the original data.

Model Evaluation

In order to assure the validity of a working model it is important to ensure that it is adequate for its intended use. Various statistical tests have been incorporated for such model evaluation, however, these equations and tests generally prove to be incapable of predicting outputs from required inputs. In practice, a test can only address the question of whether a model is invalid beyond reasonable doubt.[23] The assumptions underlying the better known statistical inference techniques are rarely met when simulating dynamic stochastic systems, as seen within the behavior of erythropoietic development and virus infection in our model.[23]

Models are not perfect and can not always mimic every aspect of biological systems. Therefore, models need only be adequate so some limitation of accuracy and precision has to be accepted.[24-25] However, the model should be consistently reproducible. Additionally, the size of the acceptable precision can be defined with

reference to the purpose of the model.[24] Kohn suggested that the ambiguous analysis and lack of sensitivity found with regression can be overcome by using the root mean square prediction error (RMSPE) [25]:

$$\text{RMSPE} = \sqrt{\left[\frac{\sum (\text{predicted} - \text{observed})^2}{\text{number of observations}} \right]}$$

This term is the square root of the estimate of variance of observed values about the predicted values.[25] The RMSPE can be separated into its constituent parts in order to identify systematic problems with the model.[25] In an earlier paper, Kohn et al. decomposed the RMSPE into two terms: the mean bias and the residual error.[25] The mean bias represents the average inaccuracy of model predictions across all data.

$$\text{Mean bias} = \frac{\sum (\text{predicted} - \text{observed})}{\text{number of observations}}$$

The residual error was then defined as the remaining error in model prediction after accounting for the mean bias.[25] This error is also referred to as prediction error excluding mean bias. The following equation is the square root of the RMSPE squared minus the mean bias squared:

$$\text{Residual error} = \sqrt{[\text{RMSPE}^2 - (\text{mean bias})^2]}$$

It was important to calculate the slopes of the red cell decline from the graphs of the real system cats and compare them to the graphs from the mathematical model. Upon first inspection, the graphs seemed to appear very different (Fig 15 and 16). The key point was to examine the slopes once EA was initiated. The Hct cell counts from each cat were graphed and the slope was calculated from these results. The slopes ranged from 0.3 to 0.929. Six of the graphs returned a slope value of 0.551 and the average of all slopes was 0.532. The decline in circulating Hct, from the model, produced a calculated slope of 0.543 and the marrow Hct declined at a slope of 0.5. When these results were used in the above formulas, the calculations were astounding. The calculation of the RMSPE, using the slope of the loss of circulating Hct to show how well the predictions fit the observed data, was found to be 0.002 or the model over predicted the loss by this negligible amount. The mean bias was calculated to 0.0004 and the residual error was the same as the RMSPE. When the slope of the marrow Hct was used the resulting RMSPE under predicted the loss by 0.006, the mean bias was found to be 0.001 and the corrected error was shown to equal 3.5×10^{-5}. While insignificant, this error represents a small difference between real-system outputs and the outputs from the computerized mathematical model. The error demonstrated that the model fit closely to the data obtained from experimentally-induced FeLV-EA. These results allow us to show conclusively that Hct declines rapidly after viral targeting of the BFU-E cell population. We further believe that this model can be expanded for the investigation of other hematopoietic queries.

CHAPTER II: FLA: The Feline Major Histocompatibility Complex

FLA

The major histocompatibility complex (MHC) is a multigene complex in mammals that includes two distinct classes of genes. The products of these genes participate in immune regulation and response to foreign antigens. Class I genes encode an approximately M_r 45,000 cell surface glycoprotein which is noncovalently associated with beta-2 microglobulin on the majority of somatic cells.[26] Class II genes encode α and β chains of a noncovalently associated heterodimeric glycoprotein expressed on the cell surface of lymphocytes and macrophages.[26] The estimated relative masses are approximately 32,000 – 35,000 for the α chain and 25,000 – 28,000 for the β chain.[26] In humans there are three functional class I genes *HLA-A, -B* and *–C* clustered on the short arm of chromosome 6.[26-29] The cat has three comparable functional class I genes, at this time loosely termed FLA –A, -B, and –C, found on the feline chromosome B2.[28]

Of the nonprimate mammalian species with developing comparative gene maps, the feline gene map displays the highest level of conservation with humans.[26, 28-30] Comparison of the FLA class I coding sequence with other class I genes from other species has revealed that domestic cats genes display 81% to 85% sequence homology with humans.[26, 28-31] Feline and human class I genes have similar sequences and protein structures, with three extracellular domains, one transmembrane domain and one cytoplasmic domain.[28] Variable codons detected in FLA class I alleles were,

in most cases, in positions that were also variable in humans.[28-30] Invariant positions with defined functional constraints were generally conserved and invariant between the two species as well.[28]

Drs. Naoya Yuhki and Stephen O'Brien, of the National Cancer Institute in Frederick, Maryland, have previously presented a comparison of several biochemical loci plus the MHC genes that are linked to chromosome B2 of the cat and chromosome 6 of man (Fig 2).[32] The homologous genes occur on both arms of human chromosome 6, supporting their proof that a large portion of that chromosome is conserved as a linkage group on cat chromosome B2.[32]

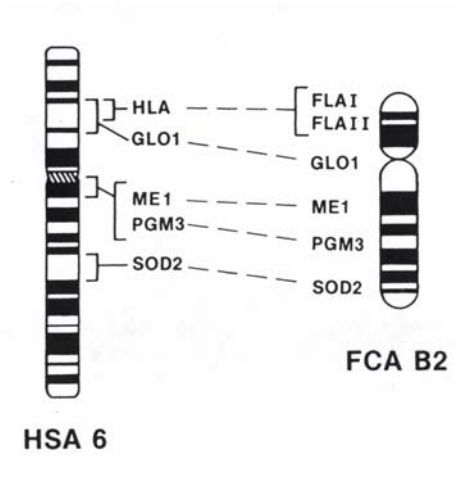

Figure 17. Comparison of the Human MHC to the Feline FLA. Diagram of the regional positions the MHC assigned to human and the domestic cat of homologous loci including chromosome 6 and their locations on the feline B2 (FCA).[32]

To detect and classify the FLA class II genes, Yuhki and O'Brien employed three types of mouse and four types of human class II DNA probes.[32] The mouse class II molecular probes, from Balb/c mice, were A^d_α, E^d_α and A^d_β.[32] The human class II molecules, used as probes, were $DPW2_\alpha$, DO_β, $DPW2_\beta$ and $DR1_\beta$.[32] DNA from eleven cats were digested with restriction enzymes and hybridized with each of the

mouse probes, while DNA from 16 cats were hybridized with the human probes. The DP_{α} and DO_{β} detected faint bands, while the DR_{β} probe gave strong and consistent bands. Neither the mouse A^{d}_{β} nor the human DP_{β} could detect any bands. From these results the group determined that FLA II has three different class II α genes: A^{d}_{α} specific, $A^{d}_{\alpha,}\, E^{d}_{\alpha}$ common (as these two probes cross-hybridized with a single gene) and DP_{α}-like genes. They also found that the FLA II has two different class II β genes, the DO_{β} and DR_{β}-like genes.[32] Since the mouse E class II gene belongs to the human DR class II gene family, it is their suggestion that the cat $A^{d}_{\alpha,}\, E^{d}_{\alpha}$ common gene may belong to the DR family.[32] This relationship between human and feline chromosomes makes the feline an attractive model for human disease.[29, 31] Dr. O'Brien and his laboratory staff have sequenced much of the feline genome, including both FLA I and FLA II. Of the 100+ disorders that have demonstrated Mendelian patterns of inheritance in cats, many pathologies are analogous to human inherited disorders and mirror the genetic locations on the genome.[30] HSC transplantation in cats should prove beneficial both for the treatment of feline disorders and the examination and possible therapy for human disorders. The awareness of the moment when the FHSC are at their highest transplantation potential, through the determination of the absence of FLA, is an important first step to their use as effective therapy.

Hematopoietic Stem Cells and Stem Cell Therapy

Hematopoietic stem cells have been studied for more than 50 years. Hematopoietic stem cell transplants (HSCT) are now routinely used to treat patients with cancers and

other disorders of the blood and immune systems. In animal studies, researchers have recently observed that HSC appear to be able to form other kinds of cells, such as muscle, blood vessels and bone.[33] It may be eventually possible to use HSC to replace a wider array of cells and tissues.

The stem cells that form blood and immune cells are the HSC. They are ultimately responsible for the constant renewal of billions of blood cells each day. The first evidence and definition of blood forming stem cells came from studies of people exposed to lethal doses of radiation in 1945.[33] In the early 1960s, Till and McCulloch began analyzing the bone marrow to find out which components were responsible for regenerating blood.[34] They defined what remain the two hallmarks of an HSC: it can renew itself and it can produce cells that give rise to all the different types of blood cells.[33-34]

Despite our experience with HSC, there are serious roadblocks to the success of their use, not only as therapy for the replacement of blood and immune cells, but in expanding their use beyond this. First, transplantation of allogeneic marrow cells from alternative donors has usually resulted in an increased incidence of graft failure and/or GVHD. These problems have depended upon the source of the graft and the use of ex vivo manipulation to deplete T-cells as prophylaxis against GVHD.[35-42] However, not only do a high percentage of patients still show signs of GVHD, but T-cell depletion increases the risks of viral infections, relapse of disease post transplant (probably due to the parallel abrogation of a potentially beneficial graft-versus-

leukemia effect) and graft rejection.[35, 38-39.41-42] Second, isolated HSCs in vitro are unable to proliferate and differentiate.

The classic source of HSC as transplant therapy has been the bone marrow. For over 40 years, bone marrow transplants (BMT) have been performed by anesthetizing the stem cell donor, puncturing a bone (typically the hip bone) and drawing out bone marrow cells with a syringe. Only one cell in 100,000 cells in the marrow is a long-term, blood forming stem cell.

Bone marrow retrieval is quickly fading, as the harvesting of donor cells from peripheral, circulating blood has now become the major source of HSCs for clinical transplantation. Only a small number of stem and progenitor cells circulate in the bloodstream. This number can be increased by injecting the donor with a cytokine, such as granulocyte-colony stimulating factor (GCSF). Of the cells collected, only 5 to, very rarely, 20 percent of these are true HSC.[33,35] Although peripherally harvested cells engraft more quickly than bone marrow, they are more likely to cause GVHD.[33,35]

Umbilical cord blood and placenta are a rich source of HSC, however they yield only a very small amount. The first successful umbilical cord blood transplants were performed in the late 80's and early 90's in children with Fanconi anemia.[43] Because the amount of cord blood collection is small, the majority of recipients receiving umbilical cord blood transplants are children.[43-44] Although GVHD incidence is

lower, this may be due in large part to the fact that children have a lower overall incidence of GVHD.[43-44] Additionally, there is evidence that maternal cell contamination exists in cord blood collections, posing a serious threat to adult recipients of cord blood transplants.[43-44]

Unlike HSCs from the other sources, fetal HSCs, before a certain gestational point, lack MHC cell surface determinants, thereby avoiding GVHD, have a greater ability to self-replicate and readily lend themselves to gene insertion and manipulations.[33,44] European researchers have shown that the relative number of CD34+ cells (a cell surface marker denoting a cell as an undifferentiated stem cell – see below) in collections declined with increasing gestational age.[45] In fact, in studies with mice, cells from fetal mice were 50 to 100 percent better at repopulating marrow than cells from either juvenile mice or young adult mice.[33]

HSC transplantation has been used for therapy against leukemia and lymphoma, inherited blood disorders, rescue in cancer chemotherapy and may be useful for other disorders such as diabetes, lupus erythematosis and rheumatoid arthritis. Currently, the use of HSCT is restricted to patients with fatal or near fatal illnesses due to the serious risks involved. These risks are GVHD, graft rejection and life threatening infections during the period before HSCs have engrafted and resumed full blood cell production. Allogeneic grafts must come from donors with a close HLA match to the patient.[44] This match is not always available and, thus, many patients are unable to benefit from HSCT. Additionally, even in patients who receive an HSCT from an

HLA-matched sibling, GVHD still poses a severe threat due to minor histocompatibility antigens and pre-treatment with immunosuppressants.[44] Therefore, the knowledge of when the MHC first appear on the surface of these cells will enable transplants to be used without the risks involved and given to a broader range of patients. The benefit of this study in cats is that they share a high genetic homology to humans. This study will not only benefit cats, but there is direct correlation to studies in humans, which will further the research of human FHSC.

Immunophenotypes of Mammalian HSC

All cellular elements of blood, including white blood cells, red blood cells, T-cells, etc., arise from a common precursor cell, the HSC. Before a certain point in human gestation, the HSC are absent of any cell surface markers.[46-47] CD34, a stem cell marker, has been identified and characterized in humans, dogs, cats and mice.[46-47] In non-human primates, monoclonal antibodies to human CD34 are cross reactive and identify a population of stem cells.[47-48] Additionally, c-kit and Ly-6A/E (or Sca-1) have been identified as stem cell markers in mice.[47,49,50,52] C-kit molecules are cell-surface receptors on bone marrow cell types that identifies HSC and mesenchymal stem cells (MSC), while Sca-1 is a cell-surface protein on bone marrow cells, indicative of HSC and MSC.[50,52] These cell surface proteins distinguish more primitive hematopietic cells from lineage-specific cells.[51-52] Other cell surface molecules, such as IL-7R are absent from the surface, as they are not expressed until the cell has been committed to a specific cell lineage.[52]

The CD34+ antigen is a 115 kDa surface glycophosphoprotein, expressed on 1-3% of normal bone marrow cells.[53] In vitro data suggest that the human bone marrow CD34+ cell compartment contains primitive multipotential hematopoietic cells, responsible for both short- and long-term repopulation.[54] In humans, the CD34+ hematopoietic stem cell surface marker begins to be expressed on the surface of lymphohematopoietic cells around the 8th week of gestation.[46] A recent study found that the development of human lymphohematopoietic stem progenitor cells may be defined by CD81, as well as CD34.[55] They found that lymphohematopoietic cells that expressed CD34^{low}CD81+ were committed to differentiation, having lost most of their long-term repopulating (LTR) potential, although cells that were CD34+ and CD81+ still had all their lymphohematopoietic properties.[55] Therefore, in addition to using the appearance of FLA on the cell surface, CD81 may serve as a marker for defining the developmental stages of lymphohematopoietic cells and may be useful in the future for determining when these cells are at their highest repopulating potential. Stem cells are very rare, representing less than 0.01% of all nucleated cells in the normal bone marrow. Based on animal experiments, the morphology of HSC is thought to be similar to that of small lymphoid cells.[56] Human HSC express the surface proteins CD34+ and c-kit and are negative for CD38 and lineage specific markers.[56] From the pluripotent progenitor HSC, more specialized progenitors are formed. Under normal conditions, the majority of stem cells are dormant (G0 phase of cell cycle). A stem cell only divides to maintain the steady state of hematopoiesis or to meet the body's demand for progenitor cells (stochastic model of hematopoiesis).[56] CD34 is expressed at highest levels on the earliest hematopoietic

cells and its surface expression dramatically decreases to undetectable levels progressively during maturation.[49,56] In addition, these stem cells retain for life the ability and option of giving rise to cells of all lineages.[33,47,49] Stem cells, from unrelated donors, can be engrafted in bone marrow of individuals whose hematopoietic cells have been depleted by disease or treatment, giving rise to the entire architecture of hematopoietic cells and this forms the basis for therapeutic bone stem cell transplantation.[33,43,47,49]

Clinical Utility of Stem Cells

One of the driving forces behind this project is the hope that fetal feline hematopoietic stem cells (FHSC), once pooled, can be used as "universal donor" cells. If the point in gestation can be determined, when FHSCs lack FLA but display a high population of CD34+ molecules on the cell surface (an indication of a lack of "self" cell- or immune- surface proteins) then these cells can be obtained from fetuses of this determined age and utilized for either gene therapy or administered where a marrow transplant is indicated but no suitable donor exists. The use of FHSC, endowed with genes to inhibit FIV replication in cats is one important study that would benefit from this proposed research, leading to an animal model for the study of effective HIV treatment strategies.

Human immunodeficiency virus (HIV) has, to date, succeeded in evading existing therapies and novel anti-viral strategies. The extraordinary survival mechanisms of the virus have allowed us to merely delay the onset of the fatal acquired

immunodeficiency syndrome (AIDS) and have dealt a devastating blow, both in terms of the loss of lives and in draining individual and government financial resources. Infection of domestic cats with feline immunodeficiency virus (FIV) provides an excellent animal model for investigating the mechanisms of pathogenesis and for the development of effective antiviral therapies and vaccines for humans infected with HIV.[57-62] FIV is associated with immunosuppression and an acquired immunodeficiency syndrome (feline AIDS). The clinical course of FIV infections parallels that seen in HIV infection.[58-62]

A number of laboratories have noted how well suited cats are for lymphohematopoietic transplant studies.[63-70] Evidence of the relative ease of acceptance of marrow grafts is seen in the lower incidence of acute or chronic graft-versus-host disease (GVHD) in cats (approximately 20% versus 50-75% in humans, dogs and primates) and reports of performing allogeneic transplants across litter-mate boundaries.[67, 71-72] One major focus of this work was to isolate these cells prior to the expression of FLA, thereby avoiding the complications of GVHD.

The ultimate goal in AIDS research is to develop effective strategies that can inhibit HIV gene expression or function and consequently limit HIV replication and AIDS pathogenesis. The following table compares and contrasts the conceptual differences between conventional drug approaches and the promise of hematopoietic stem cell gene therapy:[57]

Type of Therapy	Antiviral Drug Rx	Stem Cell Gene Rx
Life-long Administration	Yes	No
Systemic Drug Toxicity	Yes	No
Drug compliance Issues	Yes	No
Drug Cytotoxicity to Lymphohematopoietic Cells	Yes	No
Protection all Blood, Lymphoid and Macrophage Cell Lineages	No	Yes
Life-long Cellular Prophylaxis	No	?
Retrovirus Strains Become Resistant	Yes	?

Table 2. Comparison of the effects of traditional antiviral treatments versus stem cell gene therapy.

Successful introduction of foreign genes into hematopoietic stem cells, in animals, will help the design of strategies to develop targeted inhibition of HIV replication in infected individuals. Hematopoietic tissues contain small populations of primitive, totipotent stem cells capable of self-renewal and of generating committed progenitors of all the different myeloid and lymphoid compartments.[73-75] In the developing feline fetus, the liver is a primary hematopoietic organ and a rich source of HSC. The HSC are, therefore, excellent vehicles for gene therapy. Many laboratories have demonstrated successful gene transfer into hematopoietic progenitor cells. The ability to harness the power of HSC will come through avoiding problems arising from transplantations and marrow grafts. Such problems can be avoided if we know when these cells first display histocompatibility markers.

The fact that feline FHSC could demonstrate such reconstitution and serve as "universal donor" cells is a very real possibility. FHSC, before a certain gestational

age, are either only slightly endowed with major histocompatibility antigens, class I and class II, or these antigens are completely absent. As well, these cells have a high population of CD34+ molecules, indicative of hematopoietic and long-term repopulating potential.[75-77] If such a gestational time point can be determined when the FHSC are at their highest long-term marrow repopulating capacity, then these cells can be pooled and administered where a marrow transplant is indicated but no suitable donor exists.

Endowing a patient with FHSC that will provide a life-long source of lymphocytes and monocytes/macrophages, which are protected against HIV, has many advantages over existing therapies for HIV/AIDS. The ability to molecularly protect cells has been accomplished by a number of laboratories in a variety of in vitro systems.[44, 76-79] One of the impediments to applying this therapy successfully is transferring the particular protective genes into a sufficient percentage of hematopoietic stem cells. Using FHSC may allow a significant increase in the gene transfer to HSC. The establishment of a system of transplanting cats with FHSC will be a more rapid way to evaluate other in vivo combination HIV/AIDS therapies because of the fortuitous synergy of feline transplantation biology, the availability of a limitless supply of FHSC and the virologically relevant FIV model system. Therefore, it is important to determine when, in gestation, the FHSC lack the FLA cell-surface proteins and are at their highest marrow repopulating potential.

Transplantation of allogeneic marrow cells from alternative donors has usually resulted in an increased incidence of graft failure and/or GVHD, depending on the source of the graft and the use of ex vivo manipulation to deplete T-cells as prophylaxis against GVHD. [37, 44, 77-78, 80] Studies have demonstrated that an exogenous gene can be expressed in feline hematopoietic cells after reconstitution of lethally irradiated donors with retroviral-infected autologous bone marrow.[435-37, 67-68, 81] Studies of FHSC transplantation in cats can more rapidly evaluate therapeutic strategies due to the abundant supply of feline fetal hematopoietic stem cells (FHSC), assisted by the fact that cats are multiparous.

The issue of solving the problem of how to transfer genes to a miniscule subpopulation of marrow cells that, by virtue of their self-renewing pluripotentiality, are not dividing and are reluctant to accept new genes, may find the answer in the unique resource of the FHSC.[37-42, 82-83] This population of cells contains a large quantity of stem cells, lacking FLA markers. Moreover, they are receptive to gene insertion because they are dividing at a rapid rate to achieve their mandate of giving rise to a replete and functional lymphohematopoietic system by the time of paturation.[84-88]

Gene therapy using FHSC may not only hold the key to successful therapy for FIV in cats, thereby providing a model for the study of novel HIV therapies, but also may lead to the treatment of FeLV in cats. FeLV has been compared to the human retrovirus, HTLV-III, studies of which would benefit from comparative FeLV studies.

Because the virus targets the BFU-E, the transplantation of FHSC endowed with genes protected against this targeted attack, may be a very real means of inhibiting further viral replication and its ability to block red cell development.

Armed with an unlimited supply of lymphohematopoietic cells coupled with the knowledge of the sequence of the FLA, antibodies to feline CD34 and to the FLA, the determination of a gestational point, when these cells are at their highest transplantation potential, is not only possible but carries the greatest probability of success. These cells will either lack FLA or have a low percentage of FLA on their cell surface. Additionally, these cells should display a high percentage of CD34+ molecules.

The Fetal Feline Liver

During feline ontogeny, hematopoiesis commences in the yolk sac, proceeds to the liver and then relocates to the bone marrow.[89] The liver of the fetus is the primary gestational hematopoietic organ. However, before 19 days, all hematopoiesis takes place within the yolk sac.[89] While cells in the fully developed liver only display MHC I, the evolving fetal liver, at around 20 days, is composed of 80% transient hematopoietic cells that will eventually display the FLA surface proteins.[27, 32, 89] Many of the erythroid progenitor cells are already expressing their cell surface markers by the 25th day of gestation, making the majority of these cells useless as a source of a marrow transplant repopulating tool. Despite this, the liver does not take

over a large percentage of hematopoiesis until it is fully formed, which happens slowly between the 30th and 46th day of fetal development.[89]

Substantial evidence has accumulated indicating the existence of stem cells in the liver. In ontogeny, hepatoblasts have the ability to differentiate into hepatocytes and biliary cells.[89, 90-91] As the organ develops, cellular terminal differentiation occurs and there appears to be an inverse relationship between cellular differentiation and cell proliferation.[91]

However, the liver is a unique organ in the capacity to regenerate after specific forms of trauma, such as partial hepatectomy. It is unclear the quantity and form of hepatic progenitor cells which could exhibit unique characteristics promoting novel therapeutic approaches in, for example, hepatocyte transplantation, gene therapy and artificial liver assist devices.[90] Thus, the identification and characterization of fetal hepatic progenitor stem cells could have a substantial impact on current experimental therapies for human liver disease.[90-91] Additionally, information regarding the first expression of cell-surface antigens will greatly enhance the knowledge of when these fetal liver cells are at their highest therapeutic potential. Fetal liver HSC have found success in the treatment of fatal blood disorders, by transplantation of these cells into the bone marrow.[90-92] Recently researchers at the Institute of Clinical Medicine, University of Tsukuba, Ibaraki, Japan discovered that hepatic stem/progenitor cells with high proliferative potential exist in the developing mouse liver, which can be enriched by using flow cytometry.[91-92]

Determination of the Appearance of FLA on the Surface of Fetal Liver Cells

Specific Aim

What is the gestational time point when genotypically unique FLA proteins first appear on the surface of fetal feline stem cells? Does this time point coincide with the loss of the long term repopulating potential of these cells, as seen through the downregulation of CD34-like cell surface antigens?

Rationale

During fetal development, hematopoietic stem cells lose their totipotency and gain cell surface proteins and antigens that determine the cellular and organ niches they will inevitably fill. The gain and loss of these cell surface determinants occurs through an orchestration of genes in concert with the loss of naiveté of the cell. As the HSC move from the yolk sac to the liver, the production of specific blood cell types is controlled by HSC programming. While hematopoiesis takes place in the liver, some of these cells leave the liver, migrate to the bloodstream and enter the thymus as T stem cells where they eventually become T-lymphocytes. However, it is not known at what stage of fetal development these cells lose their totipotency and express antigens that show they have been constrained to a specific cell lineage. The ability of these cells to repopulate the lymphopoietic architecture from one feline to another is complicated by the expression of major histocompatibility antigens on the surface of the HSC. To pool these cells for use as a therapeutic tool it is important to know when the FLA are first expressed on the surface of HSC in the liver. This knowledge will allow future therapeutic options to avoid the complications of Graft-versus-Host-

Disease. Here we show that FLA appear on the surface of the HSC within the liver as hematopoiesis moves from the yolk-sac to the liver around day 40 in feline gestation.

Methods

Livers from 10 day-old to 60 day-old feline fetuses were obtained from ovariohysterectomies. Local veterinarians were instructed to collect gravid uteri after performing pregnant spays. The gravid uteri were placed in a sterile bag and refrigerated at -4^{o} C. Once the samples were received, the fetuses were removed from the gravid uteri and placed in formalin or the -70^{o} C freezer. Tissues (whole fetuses and fetal livers) were embedded in O.C.T. compound, frozen in liquid nitrogen and stored in -70^{o} C until they were stained. 16 gauge (16G) and 17G injection needles were blunted and sharpened with a grinding machine. The 17G needle was used to punch paraffin wax cylinders, which were 3 mm in height and 2 mm in diameter, creating a matrix of cylinders on a paraffin block. One block contained 42 cylinders, while two others contained 30 cylinders. The 16G needle was used to obtain tissue cylinders from 70 paraffin-embedded whole livers and fetuses, some of which were from the same litter. These tissue samples were injected into the blank paraffin wax block. Sections between 4-6 μm in thickness were cut using a Micron HM500 cryostat and mounted onto Superfrost® microscope slides. The smaller diameter (17G) of the needle used to punch the blank wax paraffin block allowed the bigger tissue cores to fit easily into the blank.

The expression of FLA molecules on the surface of feline fetal hematopoietic stem cells within the liver was determined using a monoclonal antibody (ovine anti-MHC I

IgG 1) in a biotin-strep-avidin immunohistochemical technique. The paraffin was removed and the slides were dehydrated in a standard technique. The slides were treated with an antigen retrieval solution (DAKOCytomation) and a biotin block prior to incubation with the primary antibody, sheep anti-MHC I IgG 1, at a concentration of 1:400. These antibodies were known to cross-react in a strong manner with feline Class I MHC antigens[93]. After rinsing, the slides were treated with the secondary antibody, mouse anti-cat, at the same concentration as the primary antibody. The slides were then exposed to a blocking reagent, enzyme and substrate and counterstained.

Results

The results revealed that the protein determinants of self recognition began to be displayed on the surface of cells, within the fetal liver, around day 40 of feline fetal gestation. As well, early analysis suggested that the expression of the MHC I increased as the fetus neared birth. The fact that MHC I was expressed at this time point was startling, given the knowledge that hematopoiesis moves from the yolk sac to the liver at that same time point.

Prior studies in our laboratory revealed that the yolk-sacs of 20-day-old fetuses contain 10 times the percentage of CD34+-like cells (HSC) than the liver of 20-day-old fetuses. The percent of CD34+-like cells in the liver increases from 0.17% in 20-day-old fetuses to 0.92% on day 30, to 4.22% on day 46%, declining to 3.81% thereafter, as the fetus nears term. The percent of MHC Class I antigens revealed that

an average 95.8% of the cells were expressing the protein by day 58 (figures 18 and 19). These results suggest that cells in the fetal liver, although containing a low percentage of HSC, may still provide enough cells to be pooled for use in transplant therapy prior to day 40.

The following figures demonstrate the results of cell staining with anti-sheep MHC class I antibodies. Figures 18 and 19 showed diffuse staining of cells within the fetal feline liver with the anti-MHC I antibody. The fetuses were around day 58 (from day 56 to day 58) of gestation in both of these photos. Figure 20 and 21 displayed the negative results of staining a fetal liver sample with the anti-sheep MHC I. The fetuses, from which these last samples were collected, were 21 and 32 days old, respectively.

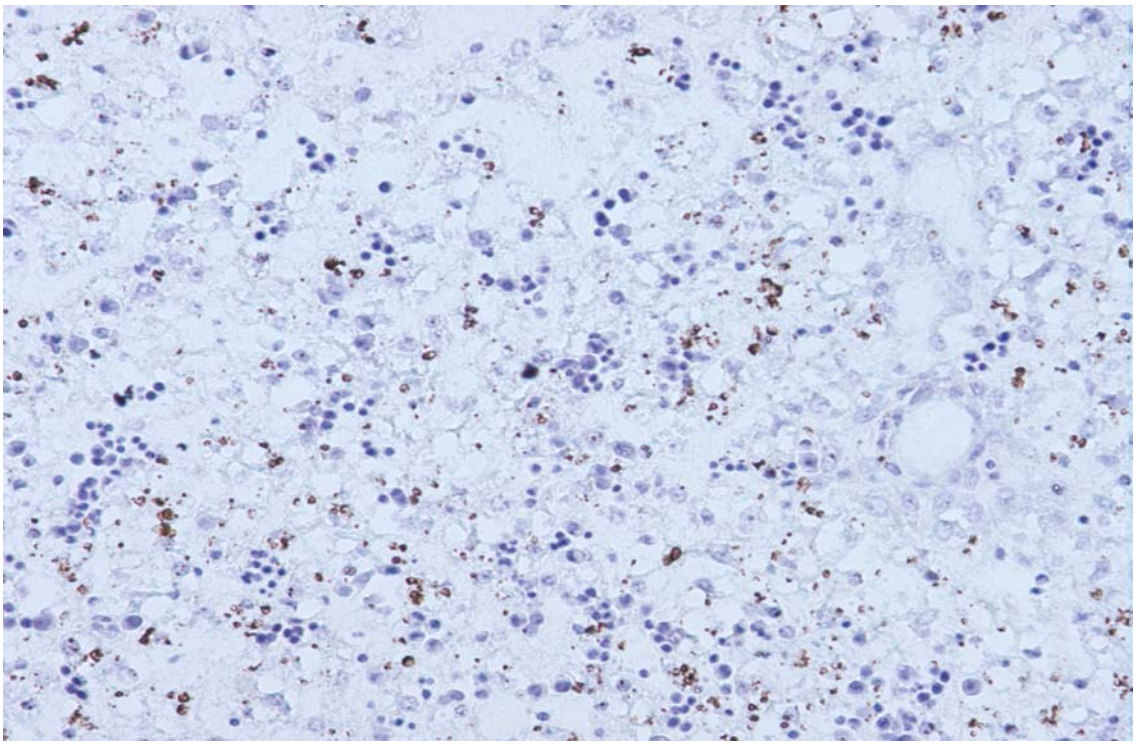

FIGURE 18. Positive results of immunohistochemical staining with anti-MHC Class I on a 58 day old feline fetal liver. A tissue array core of a fetal feline liver was stained with anti-sheep-MHC Class I. The results show diffuse staining of cells

within the liver of a 58 day old feline fetus, indicating that 94.2% of the cells were expressing MHC Class I the cell surface. Positive staining is revealed by the dark-red color seen on cells within the sample.

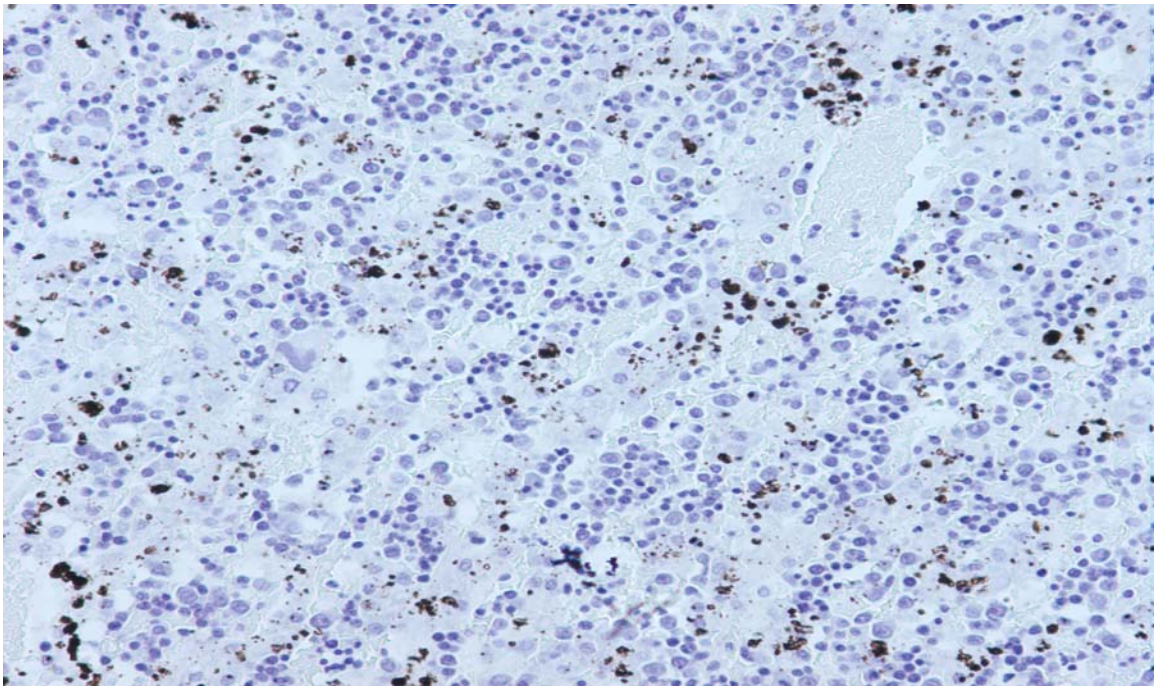

Figure 19. Positive results of immunhistochemical staining with anti-MHC Class I on a 58 day old fetal feline liver. A core sample taken from a 58 day gestational fetus was stained with anti-sheep-MHC Class I antibodies at a dilution of 1:400. The results show diffuse staining of the cells in the liver, demonstrating that 97.4% of cells were expressing MHC Class I cell surface.

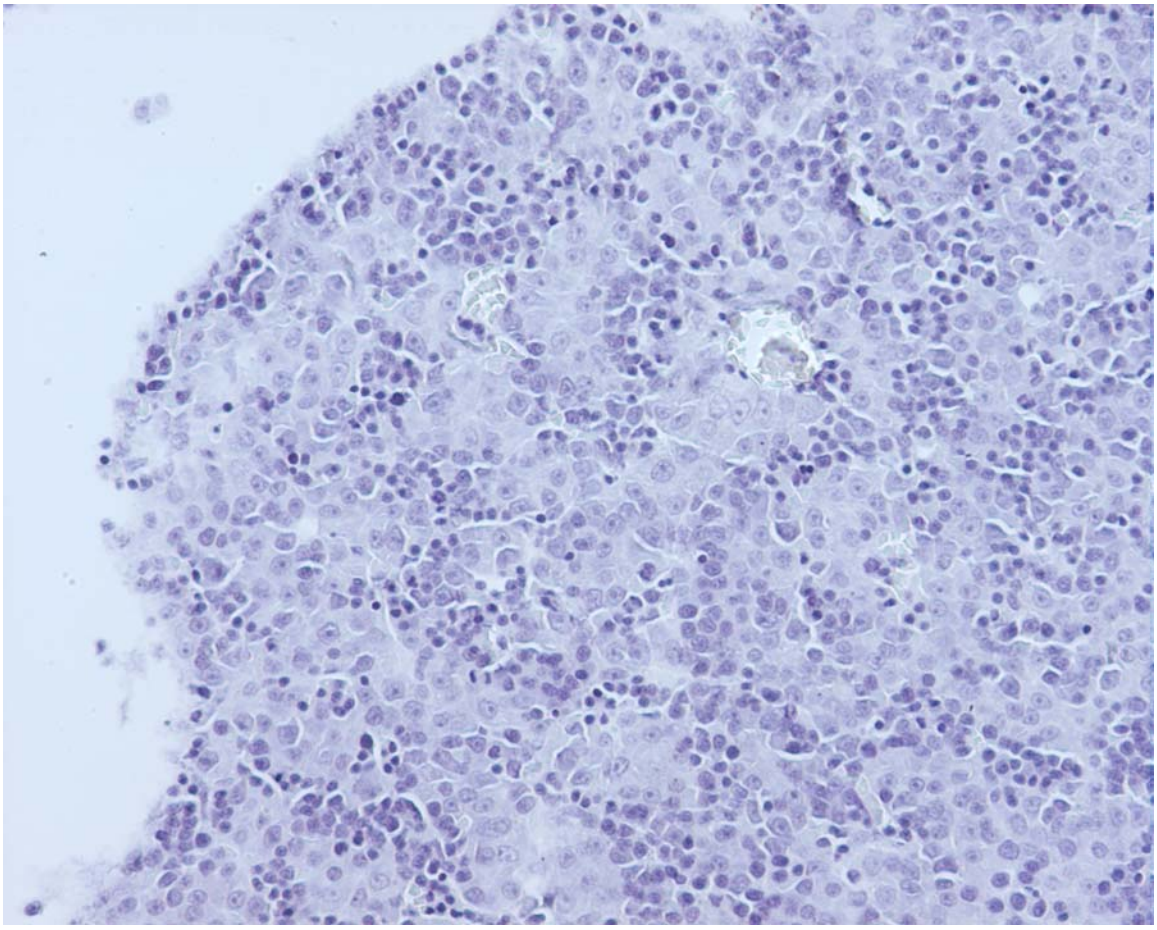

Figure 20. Negative results of immunhostochemical staining with anti-MHC Class I on cells within a feline fetal liver sample. Whole liver sample, removed from a 21 day old fetus, was stained with anti-sheep-MHC Class 1 antibodies at a dilution of 1:400. The results show that no MHC Class I proteins are expressed on cells within the fetal liver at this stage in gestation.

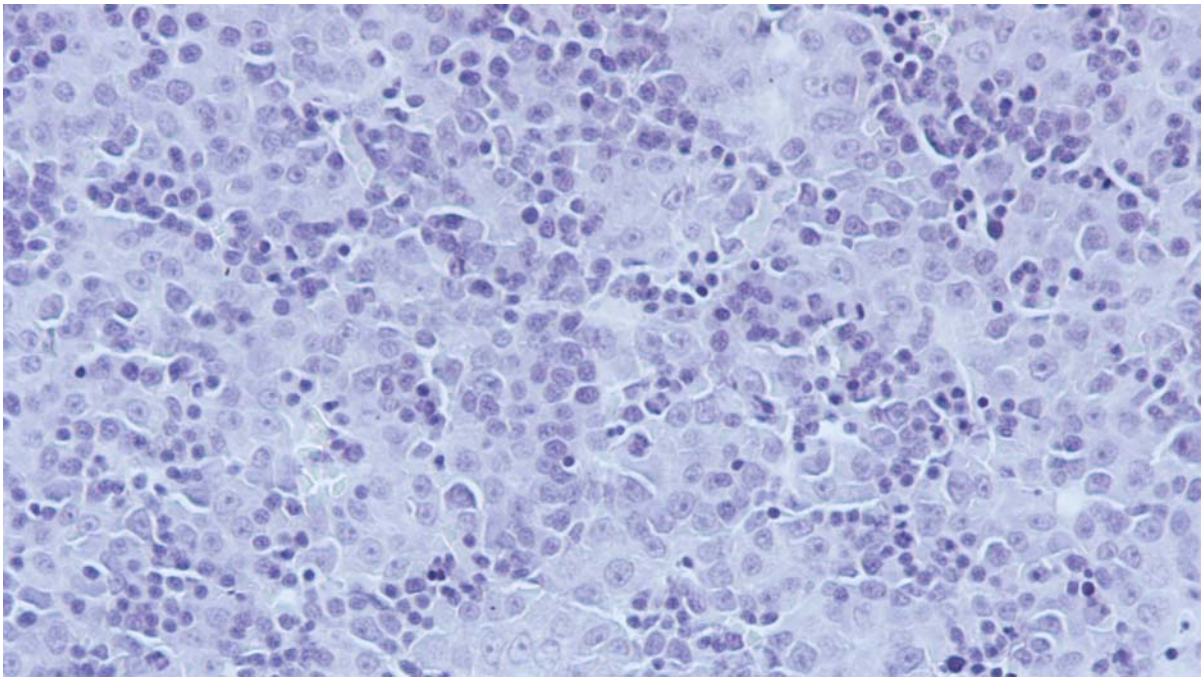

Figure 21. Negative results of immunohistochemical staining of a 32 day old feline fetal liver with anti-MHC Class 1. A tissue core sample from a 32 day old feline fetus was stained with anti-sheep-MHC Class I at a dilution of 1:400. No expression of MHC I is seen on the cells in this sample.

CHAPTER III: Feline Studies and the Relation to Human Studies

Human Immunodeficiency Virus

The research performed, herein, is both timely and topical. As the number of AIDS cases climb every year, it is clear that there is a need for a model to enable researchers to study the mechanisms of pathogenesis and have a model by which to study the development of effective antiviral therapies and vaccines. Cats are being recognized as a rich biomedical resource that has retained a high degree of genetic homology with humans than all other non-primate species. The discovery and characterization of a horizontally transmitted retrovirus (FIV) will facilitate our understanding of HIV and the therapies employed to treat AIDS, allowing researchers to help cats and humans.

Stem cell research was heralded in 1999 as the biggest scientific breakthrough of the year, holding the promise of treatments and even cures for a wide host of diseases and physically disabling conditions via HSC transplantation. Cats are well suited for HSC transplantation. They are large enough to sample while small enough to house. Feline investigations are inexpensive compared to those of other larger animal models, particularly primates. Their fastidious grooming habits and stoic temperaments are likely contributors to the lower incidence of fecal oral contamination seen in other species of HSC transplant recipients, namely canines and primates.

Similar to HIV, the FIV genome contains several open reading frames (ORFs) in addition to genes encoding the structural proteins.[93-94] These additional ORFs include

the rev and vif genes and orf A.[93-94] The FIV rev gene product is critical for virus replication.[76-77, 79, 93-94] The introductions of mutation(s) in the vif gene have revealed that this auxiliary gene product is important for efficient viral replication.[76-77, 79, 93-94] Furthermore, an unusual RNA-folding region that is required for REV (RRE) has been identified at the end of env.[76-77, 79, 93-94] This region reveals a structure that is highly conserved among several FIV isolates. FIV replication is dependent on the fully functional Rev protein and RRE for productive replication.[76, 93-94] Therefore, similar to HIV, regulatory regions and auxiliary genes of FIV can also be targeted as anti-viral strategies to inhibit virus replication.[76-78, 93-94] Since targeting multiple regions helps safeguard against viral escape mutants, the additional ORFs in the FIV genome provides multiple targets to inhibit different stages of viral replication.[93-94]

Successful introduction of foreign genes into HSCs in animals will help scientific progress toward not only developing targeted inhibition of HIV replication in infected individuals, but also treatment of genetic blood disorders and cancers of the blood. Hematopoietic tissues contain small populations of primitive, pluripotent HSCs capable of self-renewal and generating committed progenitors of all the different myeloid and lymphoid lineages.[43, 75-76] Therefore, HSCs are excellent vehicles for gene therapy.[38, 43] HSCs in the adult bone marrow are few in numbers and quiescent.[38, 75, 80] In many cases, mediated retroviral gene transduction of clonogenic progenitor cells are defined by methycellulose assays has been reported to be in the range of 2-20%.[76-78, 94] In addition, the level of gene marking drops when HSCs are maintained in long-term culture, suggesting that different populations of progenitor

cells, as defined by in vitro activity, are marked with different efficiencies.[78-79, 82, 94] In rhesus monkeys, cats and dogs reconstituted with transduced bone marrow cells, retroviral vectors have been detected in lymphoid and myeloid lineages more than one year after transplantation, suggesting successful stem cell gene transfer. Despite this, the percentage of marrow-derived cells containing the transferred gene is generally only 0.1-1%.[47-48, 63, 65, 67, 70, 94] In order for stem cell gene therapy to effectively inhibit HIV replication, a much higher percentage of stem cells must be highly stable when transferred.

Practicing veterinarians are routinely asked to perform complete ovariohysterectomies (spays) on pregnant cats or they discover a cat is pregnant while performing an elective spay. These valuable sources of FHSC are normally discarded. Having such an abundant supply of stem cells opens the door for large variety of scientific studies. FHSC before a gestational age are only slightly endowed with HLA antigens, have a high proportion of CD34+ molecules and have T-cells that exhibit thymic naïveté.[35, 73-75] These cells have been shown to elicit significantly less graft-versus-host-disease than bone marrow when used for transplantation. [35, 38-40, 42]

Graft-versus-Host-Disease and Transplant Therapy

GVHD is a serious complication that arises frequently following allogeneic HSC transplantation (HSCT). Despite all of the advances and new drug therapies, GVHD remains a major problem in children and adults. The incidence of GVHD varies from 9 to 76% and the mortality can be as high as 50%.[44] The disease occurs when T cells from donor bone marrow or peripheral blood stem cells (PBSCs) mount an

immunological attack on host tissues. GVHD classically affects the skin, liver, GI tract and the immune system.[44, 95-96] Additionally, the mucous membranes, airway and bone marrow may also be involved. The two types of GVHD, acute and chronic, are both associated with significant morbidity and mortality. Acute disease is graded from 0 (none) to IV (life-threatening).[43-44] The overall grade of GVHD predicts the clinical course and prognosis. However, even patients with a grade 0 or I only have a 56% survival rate, which decreases significantly with grades II through IV.[43-44] Adults over age 50 receiving HSCT incur GVHD at a rate of 79%.[43-44] In Japan, the incidence of transfusion-associated GVHD is estimated to be 1 in 500 open heart operations.[43-44]

Treatment for acute GVHD, which occurs within two weeks of HSCT, is usually accomplished through the use of corticosteroids and/or antithymocyte globulin, but the response rate to therapy is unsatisfactory.[95] Despite prophylaxis with cyclosporin, frequently combined with methotrexate, and use of a donor (usually a sibling) matched at the MHC gene complex, the risks for developing GVHD are quite high.[44, 95-97] In children, GVHD is responsible for one-quarter of the deaths observed after this procedure, even when stem cells from an HLA-matched sibling and prophylactic treatment are received.[95, 98]

Long term survivors of allogeneic HSCT are not free of the threat of GVHD. Chronic GVHD can develop and is the major cause of death in these individuals.[95, 99] Progressive chronic GVHD evolves directly from acute active GVHD and carries a very poor prognosis.[44, 95, 100] There is also a quiescent form of the disease, which

develops after resolution of acute GVHD.[44, 95, 99] *De novo* chronic GVHD develops without any prior history of acute GVHD.[44, 95, 99] As well, GVHD is not always due to histo-incompatibility between donor and recipient. Inappropriate recognition of self antigens can occur post HSCT, causing a GVHD-like syndrome [44, 95-96]

The agents used as therapy, against GVHD, are sadly unsuccessful and are associated with severe toxic effects. Even the new use of the macrolide antibiotic and immunosuppressant, tacrolimus, showed no improvements in overall or disease-free survival.[44, 97-100] Additionally, tacrolimus, like cyclosporin, the major drug of choice in GVHD therapy, is highly nephrotoxic.[97-98] While T cell depletion is one of the most effective means of preventing GVHD, it is associated with delayed immune reconstitution, ensuing infectious complications and, frequently, the recurrence of leukemia.[97-100] These problems are major drawbacks that can reduce or even obliterate the advantages offered by T cell depletion.[44, 97, 100] It has been observed that chronic GVHD is the main cause of morbidity and mortality in long term survivors of HSCT.[44, 96, 100]

Despite the fact that fetal stem cells can be endowed with genes to protect against various retroviral infections, these cells offer the hope of HSCT without the severe life-threatening complication of GVHD. If these cells can be pooled and used in various forms of therapy, they truly will be “universal-donor” cells. This gives hope for better HIV protection and treatment for AIDS patients.

Future Studies

Expanding the Mathematical Model

A mathematical model is a conceptual model that takes on the role of a real world problem using mathematical language, rather than ordinary languages to express a particular scientific concept. Models are necessarily simplistic descriptions of an actual context. Ordinarily, a model represents what are believed to be a few crucial features of this context and achieves simplification by omitting other aspects which are less important or are irrelevant. The danger, of course, is that something that is crucial may be left out. The obvious strengths of mathematical models are that they use mathematical languages to describe a given scientific context in the real world. This permits a high degree of precision in the statement of descriptive hypotheses or assumptions. It also facilitates the logical manipulation of the statements. Finally, it often provides quantitative (i.e., numerical) conclusions that may not be obtained if natural languages are used to describe the scientific context.

When constructing the mathematical model of FeLV-infection, it was hoped that eventually it could be expanded to produce a two-disease model, as was originally created by Dr. Irwin D. Bross. Dr. Bross developed a two-disease model of breast cancer in the 1980's, in which he used data gathered from laboratory experiments to reveal two different types of breast cancers.[101] As we know there are three forms of FeLV, it was hoped to show a two-disease model using FeLV-A and FeLV-KT to assist in determining if neutropenia and myelosuppression were direct results of the infection of the BFU-E by FeLV-KT, as secondary effects or if these were, in fact,

due to infection with FeLV, Subgroup A. We specifically hope to later expand this model to analyze real system outputs of SPF cats infected with FeLV-A. This model will then be coupled to the model for FeLV-KT to analyze the loss of white blood cells, allowing us to see if neutropenia is truly a secondary effect or if FeLV-KT must arise *de novo* with cats infected with FeLV-A.

Expanding the Antibody Studies

Human blood cells, except for erythrocytes and platelets, express CD81, a member of the transmembrane 4 superfamily (TM4SF). CD81 is also expressed on most of human immature hematopoietic cells, CD34+ cells, which are divided into three populations according to the expression of CD34 and CD81; CD34+CD81+, CD34+CD81(High) and CD34(Low)CD81+. Myeloid and lymphoid progenitors exist in the CD34+CD81+ population, and megakaryocytic progenitors are only in CD34(Low)CD81+ population. Erythroid and multipotential progenitors are shared by CD34+CD81+ and CD34(Low)CD81+ populations, but multipotential progenitors in the CD34+CD81+ population have already lost most of their myeloid potential. NK cells and mast cells can be generated from all three populations. Long-term repopulating (LTR) lymphohematopoietic stem cells are present in the CD34+CD81+ population.[102] Thus, along the differentiation cascade from $CD34^{+}CD81^{+}$ lymphohematopoietic stem cells, an up-regulation of CD81 or a down-regulation of CD34 results in a change in lymphohematopoietic properties. CD81 may serve as a marker for defining developmental stages of lymphohematopoietic stem cells.[103]

It is not known if feline lymphohematopoietic stem cells express the CD81 antigen. It is also not know how the expression of MHC I on these cells may correlate with CD81 expression. Future research is envisioned that would determine whether felines express a CD81-like antigen on the surface of lymphohematopoietic stem cells. The following questions could arise from identifying a feline CD81-like antigen:

- Is it possible to change the expression of CD81 on these cells and does such a change cause the LTR of these cells to remain high?
- Additionally, does the particular change in the regulation of CD81 effect the expression of MHC I or MHC II?
- Does the movement of hematopoiesis from the yolk sac to the liver have any effect on the expression of CD81.

The expansion of the research within this document could assist in the development of better modeling systems to determine treatment efficacy, as well as leading to more efficient, less physically-devastating treatments, overall.

References

1. **Mackey L.** 4 January 1975. Feline leukaemia virus and its clinical effects in cats. Vet. Rec. **96**(1):5-11.
2. **Cotter S.M.** 1979. Anemia associated with feline leukemia virus infection. J. Amer. Vet. Med. Assoc. **175**:1191-1194.
3. **Maggio L.** 1979. Anemia and the cat. Compendium on continuing education. **1**:114-122.
4. **Hoover, E.A., G.J. Kociba, W.D. Hardy, Jr. et al.** 1974. Erythroid hypoplasia in cats inoculated with feline leukemia virus. J. Natl. Cancer Inst. **53**:1271-1276.
5. **Mackey L, W. Jarrett, O. Jarrett, et al.** 1975. Anemia associated with feline leukemia virus infection in cats. J. Natl. Cancer Inst. **54**:209-217.
6. **Sarma P.S., T. Log.** 1973. Subgroup classification of feline leukemia and sarcoma viruses by viral interference and neutralization tests. Virology. **54**:160-169.
7. **Onions D, O. Jarrett, N. Testa, et al.** 1982. Selective effect of feline leukemia virus on early erythroid precursors. Nature **296**:156-158.
8. **Jarrett I, M.C. Goldner, S. Toth, et al.** 1984. Interaction between feline leukemia virus Subgroups in the pathogenesis of erythroid hypoplasia. Int. J. Cancer. **34**:283-288.
9. **Russell, P.H., O. Jarrett.** 1978. The occurrence of feline leukemia virus neutralizing antibodies in cats. Int. J. Cancer. **22**:351-357.
10. **Vedbrat, S.S., S. Rasheed, H. Lutz, et al.** 1983. Feline oncornavirus-associated cell membrane antigen: a viral and not a cellularly coded transformation-specific

antigen of cat lymphomas. Virology. **124**:445-461.

11. **Wichmann H-E, M. Loeffler.** 1985. Biological description of the model assumptions. In Mathematical modeling of cell proliferation: stem cell regulation in hemopoiesis, Volume I, Wichmann, H-E., Loeffler, M. eds. CRC Press, Inc., Baton Rouge, Florida. 31- 53.
12. **Wichmann, H-E, M. Loeffler.** 1985. Structure of the model. In Mathematical modeling of cell proliferation: stem cell regulation in hemopoiesis, Volume I, Wichmann, H-E.,Loeffler, M. eds. CRC Press, Inc., Baton Rouge, Florida. 55-86.
13 **Boyce, J.T., E. A. Hoover, G. J. Kociba, et al.** 1981. Feline leukemia virus-induced erythroid Aplasia: in vitro hemopoietic culture studies. Exp. Hematol. **9**:990-1001.
14. **Kawakami, T.G., G.H. Theilen, D.L. Dungworth, et al.** 1967. "C"-type viral particles in the Plasma of cats with leukemia. Science. **158**:1049-1050.
15. **Fischinger, P.J., S. Blevins, S. Normura.** 1974. Simple quantitative assay for both xenotropic murine leukemia virus and ecotropic feline leukemia viruses. J. Virol. **14**:177-179.
16 **Rojko, J.L., E.A. Hoover, S.L. Quackenbush, et al.** 1982. Reactivation of latent feline leukemia virus infection. Nature. **289**:385-388.
17 **Abkowitz, J.L., R.L. Ott, J.M. Nakamura, et al.** 1985. Feline G-6-PD cellular mosaicism: application to the study of retrovirus-induced pure red cell aplasia. J. Clin. Invest. **75**:133-140.

18. **Abkowitz, J.L., S.N. Caitlin, P. Guttorp.** 1997. Strategies for hematopoietic stem cell gene therapy: insights from computer simulated studies. Blood **89**;3192-3198.

19. **Testa, N.G., D. Onions, O. Jarrett.** 1983. Hematopoietic colony formation (BFU-E, GM-CFC) during the development of pure redcell hypoplasia induced in the cat by feline leukemia virus. Leuk. Res. **7**:103-116.

20. **Gasper, PW**. 1984. Ph.D. dissertation. Colorado State University, Fort Collins.

21. **Quigley J.G., C.C. Burns, M.M. Anderson, E.D. Lynch, K.M. Sabo, J. Overbaugh, J.L. Abkowitz.** 2000. Cloning of the cellular receptor for the feline leukemia virus subgroup c (FeLV-C), a retrovirus that induces red cell aplasia. Blood **95**:1093-9

22. **Ewen, B.S., P.W. Gasper, C.H. Pontzer, E.A. Hoover.** 2003. Mathematical Modeling of FeLV- induced EA. Submitted.

23. **Harrison, S.R.** 1990. Regression of a model on Real-system output: an invalid test of model validity. Agric. Syst. **34**:183-190

24. **Mitchell, P.L.** 1997. Misuse of regression for empirical validation of models. Agric. Syst. **54**:313-26.

25 **Kohn R.A., K.F. Kalscheur, M. Hanigan.** 1998. Evaluation of models for balancing the protein requirements of dairy cows. J. Dairy Sci. **81**:3402-14.

26. **Janeway, Jr., C.A., P. Travers, S. Hunt, M. Walport.** 1997. The induction measurement and manipulation of the immune response. *In:* Immunobiology, Austin, P., Lawrence, E., Robertson, M, eds. Current Biology, Ltd., London, and Garland Publishing, Inc., New York 2:26-2:30.

27. **Yuhki, N, G.F. Heidecker, S.J. O'Brien.** 1998. Characterization of MHC cDNA clones in the domestic cat: diversity and evolution of class I genes. J. Immunol. **142**:3676-3682.

28. **Winkler, C., A. Schultz, S. Cevario, S.J. O'Brien.** 1989. Genetic characterization of FLA, the cat major histocompatibility complex. PNAS **86**:943-947.

29. **Menotti-Raymond, M., V.A. David, L.A. Lyons, A.A. Schaffer, J.F. Tomlin, M.K. Hutton, S.J. O'Brien.** 1999. A genetic linkage map of microsatellites in the domestic cat (*Felis catus*). Genomics ;**57**:9-23

30 **Cho, K-W, H-Y Youn, M. Okuda, H. Satoh, S. Cevario, S.J. O'Brien, T. Watari, H. Tsujimoto, A. Hasegawa.** 1998. Cloning and mapping of cat (*Felis catus*) immunoglobulin and T-cell receptor genes. Immunogenetics **47**:226-233.

31. **Sprent, J.** T lymphocytes and the thymus. 1993. *In:* Fundamental Immunology, Third Edition. Paul, WE, eds. Raven Press, Ltd, New York. 75-104.

32. **Yuhki, N., S.J. O'Brien.** 1988. Molecular characterization and genetic mapping of the class I and class II MHC genes of the domestic cat. Immunogenetics **27**:414-425.

33. **Kirschstein, R., Skirboll, L.** June 2001, posting date. Stem cells: scientific progress and future research directions. Department of Health and Human Services. [Online.] http://stemcells.nih.gov/info/scireport.

34. **Till, J.E., E.A. McCulloch**. 1961. A direct measurement of the radiation sensitivity of normal mouse bone marrow cells. Radiat. Res. **14**:213

35. **Gee, AP**. 1998. Collection and processing of peripheral blood hematopoietic

progenitor cells. *In*:Blood stem cell transplantation. Reiffers, J, Goldman, JM, Armitage, JO, eds. Martin Dunitz Ltd., London. 55-68.

36. **Kernon, N.** 1994. T-cell depletion for the prevention of graft-versus-host disease. *In*: Bone marrow transplantation. Forman, SJ, Blume, KG, Thomas, ED, eds. Blackwell Scientific Publications, Boston, Mass. 124-135.

37. **Martin-Hernandez, M.P., R. Arrieta, A. Martinez, P. Garcia, V. Jimenez-Yuste, F. Hernandez-Navarro**. 1997. Haploidentical peripheral blood stem cell transplantation with a combination of CD34 selection and T cell depletion as graft-versus-host disease prophylaxis in a patient with severe combined immunodeficiency. Bone Marrow Transplant. **20**(7):797-799.

38. **Rencher, S.D., J.A. Houston, TD Lockey, JL Hurwitz.** 1996. Eliminating graft- versus-host potential from T cell immunotherapeutic populations. Bone Marrow Transplant. **18**(2):415-420.

39. **De Vreis-van der Zwann, A., M.A. van der Pol, A.C. Besseling, L.P. de Waal, C.J. Boog**. 1998. Haematopoietic stem cells can induce specific skin graft acceptance across full MHC barriers. Bone Marrow Transplant. **22**(1):91-98.

40. **Drobyski, W.R., D. Majewski.** 1996. Treatment of donor mice with an alpha-beta T cell receptor monoclonal antibody induces prolonged T-cell nonresponsiveness and effectively prevents lethal graft-versus-host disease in murine recipients of major histocompatibility complex (MHC)-matched and MHC-mismatched donor marrow grafts. Blood **87**:5355-5369.

41. **Wang, B., N.S..El-Badris, R.A. Good**. 1997. Purified hematopoietic stem cells without facilitating cells can repopulate fully allogeniec recipients across entire

major histocompatibility complex transplantation barriers in mice. PNAS **94**:14632-14636.

42. **Clark, P.A., N. Pender.** 1995. Transplantation of T-lymphocyte depleted marrow with an addback of T-cells. Hematol. Oncol. **13**:219-224.

43. **Broxmeyer, H.E**. 1998. Cord blood stem cell transplantations. *In*: Blood stem cell transplantations, Reiffers, J., Goldman, JM, Armitage, JO, eds. Martin Duntz, Ltd., London. 233-45.

44. **Chao, N.J.** 1999. Etiology of Graft-versus-Host Disease. *In:* Graft-versus-Host Disease, NJ Chao, ed., R.G. Landes, Co., Austin Texas. 1999;15-29.

45. **Surbek, D.V., C. Steinmann, M. Burk, S. Hahn, A. Tichelli, W. Holzgreve.** 2000. Developmental changes in adhesion molecule expressions in umbilical cord blood CD34+ hematopoietic progenitor and stem cells. Am. J. Obstet. Gynecol. **183**:1152-57.

46. **Kincade, P.W., J.M. Gimble.** 1993. B lymphocytes. *In:* Fundamental immunology, Paul, W.E. ed. Raven Press, Ltd., New York. 44-66.

47. **Gearges, G.E., B.M. Sandmaier, R. Storb.** 1998. Animal models. *In:* Blood stem cell transplantation, Reiffers, J., Goldman, J.M., Armitage, J.O., eds. Martin Dunitz, Ltd., London, 1-17.

48 **Berenson, R.J., R.G. Andrews, W.I. Bensinger.** 1988. Antigen CD34+ marrow cells engraft lethally irradiated baboons. J. Clin. Invest. **81**:951-955.

49 **Spangrude, G.J.** 1994. Biological and clinical aspects of hematopoietic stem cells. Annu. Rev. Med. **45**:93-104.

50. **Andrews, P., P. Anversa, N. Benvenisty, C. Bjornson, H. Blau, D. Bodine, et al.** June 2001. Appendix E: Markers: how do researchers use them to identify stem cells. Stem cells: scientific progress and future research directions, Department of Health and Human Services. [Online.] http://www.nih.gov/news/stemcell/scireport.htm

51 **Li, C.L., G.R. Johnson.** 1992. Long-term hemopoietic repopulation by Thy-11^{o}, Lin-, Ly6A/E+ cells. Exp. Hematol. **20**:1309-1315.

52 **Lyman, S.D., S.E.W. Jacobsen.** 1998. c-Kit ligand and flt-3 ligand: stem/progenitor cell factors with overlapping yet distinct activities. Blood **91**:1101-1134.

53. **Kraus, D.S., M.J. Fackler, C.I. Civin, W. May Stratford.** 1996. CD34: structure, biology, and clinical utility. Blood **87**:1-13.

54. **Srour, E.F., J.E. Brandt, R.E. Briddell.** 1991. Human CD34(+) HLA DR(-) bone marrow cells contain progenitor cells capable of self-renewal, multilineage differentiation, and long-term in vitro hematopoiesis. Blood Cells **17**:287-295.

55. **Ma, F., M. Wada, H. Yoshino, Y. Ebihara, T. Ishii, A. Manabe, R. Tanaka, T. Maekawa, M. Ito, H. Mugishima, S. Asano, T. Nakahata, K. Tsuji.** 2001. Development of human lymphohematopoietic stem and progenitor cells defined by expression of CD34 and CD81. Blood **97**:3755-3762.

56. **Munker, R., E. Hiller, R. Paquette.** 2001. Basic biology of hemopoiesis. *In:* Modern hematology: biology and clinical management. Munker, R, Hiller, E, Paquette, R. eds. Humana Press, Totowa, NJ. 1-18.

57. **Mergia, A., Heinkelein, M.** Foamy Virus Vectors. Curr. Top. Microbiol.

Immunol. In press.

58. **Ackley, C.D., J.K. Yamamoto, N. Levy, N.C. Pedersen, M.D. Cooper.** 1990. Immunological abnormalities in pathogen free cats experimentally infected with feline immunodeficiency virus. J. Virol. **62**:5652-5655.

59. **Davidson, M.G., J. Rottman, R.V. English, M.R. Lapin, M.B. Tompkins.** 1993. Feline immunodeficiency virus predisposes cats to acute generalized toxoplasmosis. Am. J. Pathol. **143**:1486-1497.

60. **McCheney, M.B., M.B.A. Oldstone.** 1989. Virus induced immunosuppression: infection with measles virus and human immunodeficiency virus. Adv. Immunol. **45**:335-380.

61, **Pedersen, N.C., E.W. Ho, M.L. Brown, J.K. Yamamoto.** 1987. Isolation of a T-lymphotropic virus from domestic cats with an immunodeficiency-like syndrome. Science. **235**:790-793.

62. **Pedersen, N.C., J.K. Yamamotot, T. Ishida, H. Hanson.** 1989. Feline immunodeficiency virus infection. Vet. Immunol. Immunopathol. **21**:111-129.

63. **Colgan, S.P., M.A. Thrall, P.W. Gasper, B.J..Rose, R. Fulton, A-M.B Blancquaert, W.J. Bruyninckx**. 1991. Restoration of neutrophil and platelet function in feline Chediak-Higashi syndrome of bone marrow transplantation. Bone Marrow Transplantation **7**:365-374.

64. **Dial, S.M., T. Byrne, M. Haskins, P.W. Gasper, B. Rose, D.A. Wenger, M.A. Thrall.** 1997. Urine glycosaminoglycan concentrations in mucopolysaccharidosis VI-affected cats following bone marrow transplantation or leukocyte infusion. Clinica. Chimica. Acta. **263**:1-14.

65 **Gasper, P.W., D.K. Rosen, R. Fulton.** 1996. Allogeneic marrow transplantation for a cat with acute mylogenous leukemia. J. Am. Vet. Med. Assoc. **208**:1280-1284.

66. **Norrdin, R.W., S.J. Simske, S. Gaarde, J.D. Schwardt, M.A. Thrall.** 1995. Bone changes in mucopolysacchardosis VI in cats and the effects of bone marrow transplantation: mechanical testing of long bones. Bone **17**:485-489.

67. **Cain, J.L., G.R. Cain, J.M. Turrel, G.H. Theilen.** 1990. Clinical and lymphohematologic responses after bone marrow transplantation in sibling and unrelated donor-recipient pairs of cats. Am. J. Vet. Res. **51**:839-844.

68. **Gengozian, N., L. Reyes, R. Pu, B.L. Homer, F.J. Bova, J.K. Yamamoto.** 1997. Fractination of feline bone marrow with the soybean agglutinin lectin yields populations enriched for erythroid and myeloid elements: transplantation of soybean agglutinin-negative cells into lethally irradiated recipients. Transplantation **64**:510-518.

69. **Haskins, M.E., J.A. Wortman, S. Wilson.** 1984. Bone marrow transplantation in the cat. Transplantation **37**:634-636.

70. **Prummer, O., A. Raghavachar, C. Werner, W. Calvo, F. Carbonell, I. Steinbach, T.M. Fliedner.** 1985. Fetal liver transplantation in the dog. Restoration of hemopoiesis with cryopreserved fetal liver cells from DLA-identical siblings. Transplantation **39**:349-355.

71. **Shacklett, B.L., P.A. Luciw**. 1994. Analysis of the vif gene of feline immunodeficiency virus. Virology **204**:860-867.

72. **Stead, R.B., W.W. Kwok, R. Strob, A.D. Miller.** 1988. Canine model for gene

therapy: inefficient gene expression in dogs reconstituted with autologous marrow infected with retroviral vectors. Blood **71**:742-747.

73. **Shields, L.E., R.G. Andrew.** 1998. Gestation age changes in circulating CD34+ hematopoietic stem/progenitor cells in fetal cord blood. Am. J. Obstet. Gynecol. **178**:931-937.

74. **Lim, F., J. Beckloven, A. Brand, J. Kluin-Nelemans, J. Hermans, R. Willemze, H. Kanai, J. Fallenburg.** 1999. The number of nucleated cells reflects the hematopoietic content of umbilical cord blood for transplantation. Bone Marrow Transplant. **24**:965-970.

75. **Nieto, Y., E.J. Shpall**. 1998. CD34+ blood stem cell transplantation. *In*: Blood stem cell transplantation. Reiffers, J, Goldman, JM, Armitage, JO, eds. Martin Dunitz, Ltd., London. 187-196.

76. **Bahner, L., K. Kearns, Q.L. Hao, E.M. Smogorzewska, D.B. Kohn.** 1996. Transduction of human CD34+ hematopoietic progenitor cells by a retroviral vector expressing an RRE decoy inhibits human immunodeficiency virus type I replication in myelomonocytic cells produced in long-term culture. J. Virol. **70**:4352-4360.

77. **Bonyhadi, M.L., K. Moss, A. Voytovich, J. Auten, C. Kalfoglou, I. Plavec, S. Forestell, L. Su, E. Bohnlein, H. Kaneshima.** 1997. RevM10-expressing T cells derived in vivo from transduced human hematopoietic stem-progenitor cells inhibit human immunodeficiency virus replication. J. Virol. **71**:4707-4716.

78. **Rosenzweig, M., D.F. Marks, D. Hempel, J. Lisziewicz, R.P. Johnson.** 1997. Transduction of cd34+ hematopoietic progenitor cells with an anti-tat gene

protects T-cell and macrophage progeny from AIDS virus infection. J. Virol. **71**:2740-2746.

79. **Su, L., R. Lee, M. Bonyhadi, H. Matsuzaki, S. Forestell, S. Escaich, E. Bohnlein**. 1997. Hematopoietic stem cell-based gene therapy for acquired immunodeficiency syndrome: efficient transduction and expression of RevM10 in myeloid cells in vivo and in vitro. Blood **89**:2283-2290.

80. **Wagner, J.E., J. Rosenthal, R. Sweetman.** 1996. Successful transplantation of HLA-matched and HLA-mismatched umbilical cord blood from unrelated donors: analysis of engraftment and acute graft-versus-host disease. Blood **88**:795-802.

81. **Abkowitz, J.L., M.T. Persik, G.H. Shelton, R.L. Ott, S.N. Caitlin, P. Guttorp.** 1995. Behavior of hematopoietic stem cells in a large animal. PNAS **92**:2031-2035.

82. **Lothrop, C.D., Z.S. Al-Lebban, G.P. Niemeyer, J.B. Jones, M.G. Peterson, J.R. Smith, H.J. Baker, R.C. Morgan, M.A. Eglitis, W.F. Anderson.** 1991. Expression of a foreign gene in cats reconstituted with retroviral vectors infected autologous bone marrow. Blood **78**:237-245.

83. **Johnson, C.M., D.W. Selleseth, M.N. Ellis, T.A. Childers, M.B. Tompkins.** 1994. Feline lymphoid tissues engrafted into scid mice maintain morphologic structure and produce feline immunoglobulin. Lab. Anim. Sci. **44**:313-318.

84. **Baum, C.M., L.L. Weissman, A.S. Tsukamoto, A.M. Buckle, B. Peault.** 1992. Isolation of a candidate human stem-cell population. PNAS **89**:2804-2808.

85. **Humeau, L., C. Chabannon, M.T. Firpo, P. Mannoni, C. Bagnis, M.G.**

Roncarolo, R. Namikawa. 1997. Successful reconstitution of human hematopoiesis in the SCID-hu mouse by genetically modified, highly enriched progenitors isolated from fetal liver. Blood **90**:3496-3506.

86. **Jordan, C.T., C.M. Astle, J. Zawadzki, K. Mackarehtschian, I.R. Lemischka, D.E. Harrison. 1995.** Long-term repopulating abilities of enriched fetal liver stem cells measured by competitive repopulation. Exp. Hematol. **23**:1011-1015.
87. **Morrison, S.J., H.D. Hemmati, A.M. Wandycz, I.L. Weissman.** 1995. The purification and characterization of fetal liver hematopoietic stem cells. PNAS **92**:10302-10306.
88. **Rebel, V.I., C.L. Miller, C.J. Eaves, P.M. Lansdorp.** 1996. The repopulation potential of fetal liver hematopoietic stem cells in mice exceeds that of their liver adult bone marrow counterparts. Blood **87**:3500-3507.
89. **Gasper, P.W.** 2000. The hematopoietic system. *In:* The fifth edition of Schalm's veterinary hematology. Feldman, B.F., Zinkl, J.G., Jain, N.C., eds. Lippincott, Williams & Wilkins, Philadelphia, PA.
90. **Feldman, G.** 2001. Liver transplantation of hepatic stem cells: potential use for treating liver diseases. Cell Biol. Toxicol. **17**:77-85.
91. **Zanjani, E.D., J.L. Ascensao, M. Tavassoli.** 1992. Homing of liver-derived hemopoietic stem cells to fetal bone marrow. Trans. Am. Phys. **105**:7-14.
92. **Suzuki, A., Y.W. Zheng, K. Fukao, H. Nakauchi, H. Taniguchi.** 2001. Clonal expansion of hepatic stem/progenitor cells following flow cytometric cell sorting. Cell Transplant. **10**:393-396.

93 **Park, J., P.E. Nadeau, A. Mergia.** 2002. A Minimal Genome Simian Foamy Virus Type 1 (SFV-1) Vector System with Efficient Gene Transfer. Virology. **302**:236-244.

94. **Zucali, J. R., T. Ciccarone, V. Kelley, C.M. Johnson, A. Mergia**. 2002. Transduction of Umbilical Cord Blood CD 34+ NOD/SCID Repopulating Cells by Simian Foamy Virus Type 1 (SFV-1) Vector. Virology. **302**:229-335.

95. **Bishop, S.A. *et al.*** 1996. Vaccination with fixed feline immunodeficiency virus (FIV) infected cells: protection, breakthrough and specificity of response. Vaccine **14**:1243-50.

96 **Smith, BR**. 1997. Stem cell transplantation. *In:* Cancer principles and practice of oncology, 5th ed. DeVita Jr., VT, Hellman, S, Rosenberg, SA, eds. Lippincot-Raven, Philadelphia, PA. 2621-39.

97. **Lee, J.W., H.J. Deeg.** 1997. Choosing a regimen for prophylaxis of graft-versus-host disease. BioDrugs. **7**:15-22.

98. **Plosker, G.L., L.B. Barradell.** 1996. Cyclosporin: a review of its pharmacological properties and role in the management of graft versus host disease. Clin. Immunother. **5**:59-90

99. **Barrett, J**. 1992. Graft-versus-host disease. *In:* Bone marrow transplantation in practice, Barrett, J, Treleaven, J, eds. Churchill Livingstone, London. 257-72.

100. **Zecca, M, F. Locatelli.** 2000. Management of graft-versus-host disease in paediatric bone marrow transplant recipients. Paediatr. Drugs. 2:29-55.

101. **Bross I., L. Blumenson, N. Slack, R. Priare.** 1968. A Two-Disease Model for Breast Cancer. ***In:*** *Prognostic Factors in Breast Cancer*, (A.P.M. Forrest and P.

B. Kunkler, eds.) E.& S. Livingstone, Edinburgh, Scotland.

102. **Tsuji K., M.A. Feng, D. Wang.** 2 December 2002. Development of human lymphohematopoiesis defined by CD34 and CD81 expression. Leuk Lymphoma. **43**(12):2269-73.

103. **Ma, F.**, **M. Wada**, **H. Yoshino**, **Y. Ebihara**, **T. Ishii**, **A. Manabe**, **R. Tanaka**, **T. Maekawa**, **M. Ito**, **H. Mugishima**, **S. Asano**, **T. Nakahata**, **K. Tsuji.** 15 June 2001. Development of human lymphohematopoietic stem and progenitor cells defined by expression of CD34 and CD81. Blood. **97(**12):3755-3762